Eidgenössische Technische Hochschule Zürich
Swiss Federal Institute of Technology Zurich

Institut für
Technische Informatik und
Kommunikationsnetze

Harvesting-Based DPP for Indoor Environmental Monitoring

Semester Project

Luca Rufer
lrufer@student.ethz.ch

Computer Engineering and Networks Laboratory
Department of Information Technology and Electrical Engineering
ETH Zürich

Supervisors:
Naomi Stricker
Reto Da Forno
Dr. Andres Gomez
Prof. Dr. Lothar Thiele

January 30, 2022

Acknowledgements

I would like to thank the Computer Engineering Group (TEC) and especially my supervisors Reto Da Forno, Dr. Andres Gomez and Naomi Stricker for making this Semester Project possible. Thank you for the tremendous help on the design and production of the prototype, and all the time you invested in software and helping me to assemble and test everything.
I also want to thank my friends at Swissloop for supporting me with ideas, materials and tools during this project, especially my good friend Philip Wiese. The many conversations we had allowed for great advancements in the project.

Abstract

With the rise of wireless sensor networks for environmental monitoring applications, the need to power such networks with low-cost, low-maintenance and environmentally-friendly energy source arises. In this project, such a sensing platform powered by solar harvesting is developed. To supply the platform with power during short night periods where no energy can be harvested, the platform is equipped with a small energy storage component. The platform senses environmental conditions like CO_2 and volatile organic compound (VOC) concentration and processes the collected data. The platform is capable of short-range communication using Bluetooth Low Energy (BLE) and long-range communication using LoRa. Different operation modes allow the platform to dynamically adapt its power consumption depending on the available energy. The current consumption in its lowest power mode was measured to be 8.21 µA, and with periodic BLE messages, an average consumption of 18.6 µA was recorded. With these characteristics, this project will serve as an experimental platform for research on advanced gas sensing and energy-aware synchronous communication.

Contents

List of Figures

List of Tables

Chapter 1

Introduction

With the rise of IoT-devices in Industry 4.0 and smart homes, the desire to collect data increases more and more. For many applications like smart building control and environmental monitoring of workplaces, the collection of data is a prerequisite for efficient and effective monitoring and control. With a distributed network of sensing nodes, data can be collected to improve systems like heating and ventilation. With these improvements, the amount of energy wasted can be reduced and working and living conditions can be improved, benefiting residents, the workforce and the environment.

Most of the sensing platforms used today are either directly powered by the grid or powered by batteries. Platforms that are powered by the grid are inflexible in installation whereas platforms powered by batteries are often bulky and maintenance-intensive. As an alternative to such platforms, harvesting-based platforms are regarded to be scalable, easy to use and environmentally-friendly. Platforms that use indoor harvesting can tap into an inexhaustible power-source. However, the amount of available energy is very low and highly volatile, as the available light can suddenly change with a flip of a switch. This leaves many design challenges that must be solved when attempting to power sensing platforms from such a variable, low-power energy source. To solve this, the sensor node needs to be able to dynamically adjusts its power consumption depending on the currently available power, and possibly also on predictions of the power available in the future. The platform can only be operated robustly and long-term if its sub-systems manage the available energy efficiently to perform their tasks.

A sensor node typically has three tasks: sensing, processing, and communication. For all of these three tasks, there are different challenges to achieve dynamically adjustable low power consumption. In this project, a platform is developed to test software algorithms for energy-aware sensing, processing, and communication by creating a harvesting-based platform with advanced gas sensors, a powerful low-power micro controller for data processing and various capabilities for wireless communication. This project is a step towards a robust sensing platform and will be used as an experimental platform for research on advanced gas sensing and energy-efficient synchronous communication.

Chapter 2

Background

The TEC at Eidgenössische Technische Hochschule Zürich (ETHZ) conducts research in many areas of computer engineering and embedded system design. Among these areas of research are energy harvesting, low-power sensing and communication, which are relevant for this project. The research done by TEC and other groups at associated universities provide the background for this project. While these areas of research are very wide, a relevant example of past or ongoing research is provided here for each area to provide the necessary insights for this project.

2.1 MiroCard

The MiroCard [1] is a batteryless smart card powered by solar harvesting. It serves as an on-demand BLE beacon, and has high processing and memory availability compared to traditional Radio Frequency Identification (RFID) smartcards, even enough for modern secure communication protocols. The MiroCard demonstrates the feasibility of solar-powered batteryless processing platforms with wireless communication capabilities.

2.2 DPP

The Dual Processor Platform (DPP) architecture [2], developed by TEC, it builds upon the design practice to isolate different tasks of a system onto different microcontrollers, like dividing a system into an application processor for sensing, processing and actuation, and a communication processor for wireless communication. The authors suggest using an additional processor as an interconnect for asynchronous message passing. For this interconnect, the authors created BOLT. The asynchronous separation allows for predictable run-time behaviour of the application and communication processor and strict decoupling of power, clock and time domains. Notable advantages of such an architecture are the

modularity, possibility for parallel software design and independent power management for the two processors. The disadvantage however is the increased cost and space requirement for the three microcontrollers.

2.2.1 BOLT

BOLT [3] is the asynchronous processor interconnect developed for the DPP architecture to pass messages between microcontrollers. For each of the microcontrollers, BOLT has a First-In-First-Out (FIFO) queue where messages are stored until they are retrieved by the receiver. BOLT is implemented on an MSP430FR5969 Microcontroller Unit (MCU) with non-volatile Ferroelectric Random-Access Memory (FRAM) memory. The non-volatile memory allows BOLT to be powered down without risking to lose a message. For each of its two communication partners, BOLT uses a Serial Peripheral Interface (SPI) interface and four control signals. BOLT is designed for ultra-low-power consumption with a drain current down to 430 nA during periods of inactivity.

2.2.2 Flora

Flora [4] is a software library developed by TEC at ETHZ for the DPP2 Lora ComBoard [5]. It contains implementations of wireless protocols like DiscoSync [6], Low-Power Wireless Bus [7], Event-triggered Low-Power Wireless Bus [8] and Gloria [5]. It is designed to run on an STM32L4 MCU and also handles the low-level communication to the SX1262 used as the LoRa transceiver.

2.3 Gas Sensing

On the global sensors market, a wide range of gas sensors are available. Metal-oxide-based sensors are a popular choice for low-power gas sensors. These types of sensors operate a heat-plate at high temperatures, which requires a lot of energy. In [9], the energy consumption of the sensor is reduced by duty-cycling it. This duty cycling however results in long cold start times, poor transient responses and changes in the sensor's sensitivity profile. The authors of [9] manage to improve these characteristics again using machine learning and predictive sensing. Additionally, they simulate that it is possible to operate power-intensive sensors like the SGP30 using only indoor photovoltaic harvesting, when duty cycling is used. This technique requires significant memory and computation power to execute the neural network, which a new platform for such research must support.

Chapter 3

Architecture

The goal of this project is to design a platform which can be used for a wide range of research applications in the domains of energy harvesting, wireless communication networks and gas sensing. The architecture is divided into four parts. A separate subsystem is designated to each of the above mentioned three areas of research. An MCU is used to collect, process and distribute information between the other subsystems, and it features peripherals to provides direct feedback to the user. This MCU is referred to as the application processor. An overview of the interaction of these parts can be found in Figure 3.1.

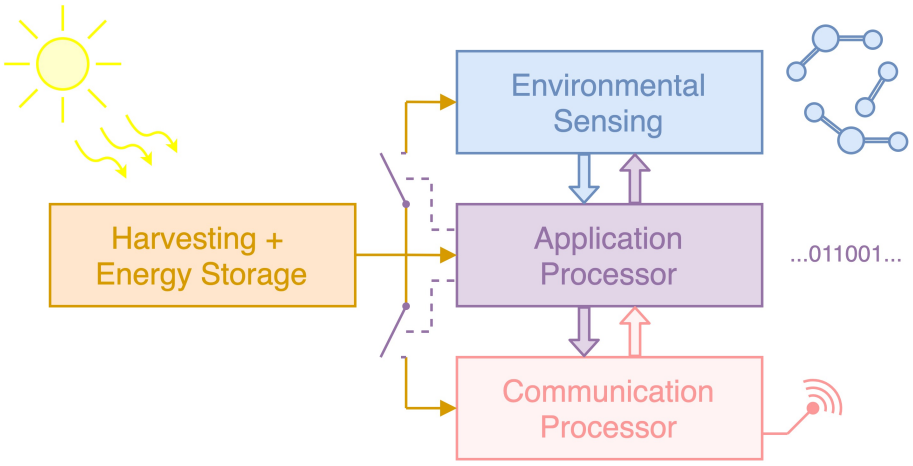

Figure 3.1: Overview of the System Architecture

The Harvesting and Energy Storage subsystem is used to provide power to the platform. In order to control the power consumption of the platform, the energy consumers are split into three power domains: power domain 0 contains the application processor, power domain 1 contains the environmental sensors for the gas sensing and power domain 2 contains the wireless communication. The power domains 1 and 2 can be enabled and disabled by the application processor, power domain 0 is always on, as long as the storage element has enough energy to

supply it. In the next four sections, the architecture of each of these subsystems is discussed individually.

3.1 Harvesting and Energy Storage

As the name indicates, the harvesting circuit is used to harvest energy from its surroundings. This subsystem is composed of multiple sequential stages, as shown in Figure 3.2.

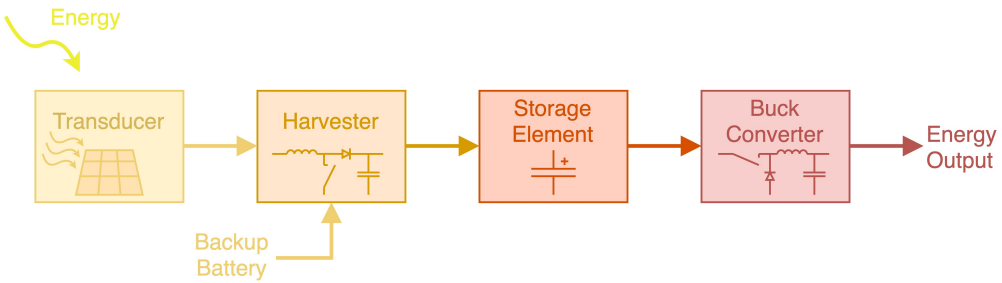

Figure 3.2: Overview of the Harvesting and Energy Storage Subsystem

In the first stage, the transducer converts energy from the environment into electrical energy. The harvester then uses the electrical energy provided by the transducer to monitor and charge a storage element. As the voltage of a typical electrical energy storage element varies with the charge level, a buck converter is then used to generate a constant output voltage for the remaining circuitry of the board.

To make the energy supply of the harvesting circuit more reliable, an external power source like a battery can be connected as back-up to keep the storage element at a minimum charge level in case no energy can be harvested for a long period of time.

3.2 Wireless Communication

For the wireless communication, the board uses a transceiver that supports both Frequency-shift keying (FSK) and LoRa modulation to enable efficient short-range as well as long-range communication. The control of the wireless communication is not implemented on the application processor, but on a separate MCU called the communication processor, using the architecture described in [2]. This allows easier resource management and software development, as the platform control and communication control don't have to share execution time or peripherals. To allow message passing between the communication processor

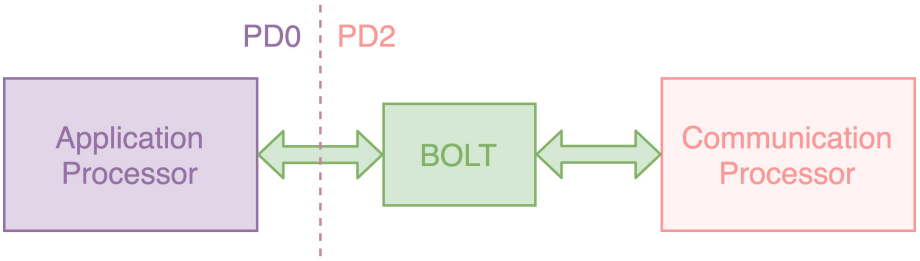

Figure 3.3: Processor Interconnect

and the application processor the system uses BOLT[3] to create a stateful processor interconnect. To implement BOLT, an additional MCU with non-volatile memory is placed between the two processors, as shown in Figure 3.3. Both the BOLT MCU and the communication processor are located in power domain 2.

3.3 Environmental Sensing

The goal of the environmental sensing is to monitor an indoor environment and collect data. The most basic environmental quantities are temperature, humidity and air quality, and thus the platform requires sensors to measure them. For the harvesting part of the platform, it is useful to collect data of the illumination of the solar panel. As mentioned in the architecture overview, the sensors are located in a separate power domain, so they can be disabled when they are not needed.

3.4 Application Processor

The application processor is used to tie the harvesting, wireless communication and the environmental sensors together. The main tasks of the application processor are the following:

- Energy storage measurements: The state of charge of the energy storage component is measured to allow for energy-aware sensing, processing and communication.
- Power distribution control: As described in the beginning of this chapter, the energy consumers are divided in three power domains. The application processor can directly enable and disable power distribution to power domains 1 and 2, where the sensors and wireless communication reside, respectively. The application processor itself resides in power domain 0 and directly controls all components in its own power domain for low power consumption.

- Sensor control and readout: The application processor directly controls the environmental sensors and collects the measurement data.
- Control of wireless communication: The application processor has to interact with BOLT to communicate with the Communication processor to send and receive data.
- User feedback: The application processor is also responsible to provide direct user feedback. What information is provided to the user depends on what the platform is used for and differs depending on the application.

Chapter 4

Implementation

This chapter shows the implementation of the architecture explained in the previous chapter. To accommodate all the components, a custom Printed Circuit Board (PCB) was designed. It measures 72 mm by 65 mm and is slightly larger than a credit card. With all components mounted, it has a height of 10.5 mm. The top and bottom view of the PCB can be seen in Figure 4.1a and Figure 4.1b, respectively. Additionally, Figure 4.2 shows the division of the components into the four subsystems. The main objective of the design implementation is to achieve a low-power design by selecting components with low quiescent and active power consumption. The design also focuses on making the board configurable and providing access to signals and power domains via pin headers. A secondary goal was to keep the dimensions of the PCB as small as possible and retain a thin profile with the components mounted.

(a) Top View (b) Bottom View

Figure 4.1: Implementation of the Design

First, the implementations of the four subsystems described in the architecture are explained individually. After that, the theoretical current consumption and operation modes of the platform are presented.

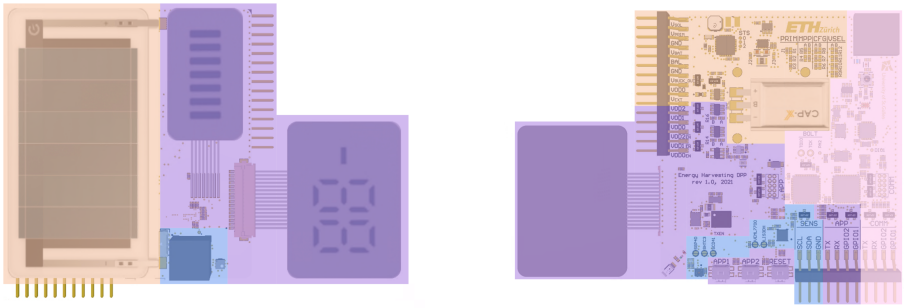

(a) Top Side (b) Bottom Side

Figure 4.2: Subsystems of the Board: Harvesting (Orange), Application (Purple), Communication (Pink) and Sensing (Blue)

4.1 Harvesting and Energy Storage

The harvesting and energy storage components are prominently visible on both sides of the board. As the board was primarily designed for stationary indoor use, a solar panel was chosen as the energy transducer. The solar panel mounted on the top side of the PCB is a 6-cell organic indoor light energy harvesting module [10] with an active area of 15 cm^2. The harvesting Integrated Circuit (IC) is an E-Peas AEM10941 with integrated boost converter to charge and monitor the energy storage element. As the board was designed to be highly configurable, it includes configurations to set the Maximum Power Point Tracking (MPPT) for the solar panel, the maximum charge and discharge voltages of the energy storage component and settings for an optional external backup battery. These settings can be changed using configuration resistors on the board, which are located on the top center on the back side of the PCB. The optional external battery, as well as other transducers or energy storage components, can be connected to the board using pin headers. The buck converter selected for the board is a Texas Instruments (TI) TPS62740 and has a configurable output voltage between 1.8 V and 3.3 V, in steps of 100 mV. Equivalent to the other configurations, the output of the buck converter can also be adjusted using configuration resistors.

Table 4.1: Energy Storage Components

Part	Manufacturer	Capacity	V_{min}	V_{max}
GA209F	CAP-XX	90 mF	0 V	5.5 V
DMT3N4R2U224M3DTA0	CAP-XX	220 mF	0 V	4.2 V
ITX121010A (2s config.)	ITEN	100 µAh	3 V	5.4 V

The PCB provides footprints for the three energy storage components listed in Table 4.1. The first two components are super-capacitors, and the third one

Table 4.2: Maximum usable Energy of Storage Components

Part	Capacity	$V_{min,eff}$	$V_{max,eff}$	E_{usable}
GA209F	90 mF	1.925 V	4.5 V	0.744 J
DMT3N4R2U224M3DTA0	220 mF	1.925 V	4.12 V	1.460 J
ITX121010A (2s config.)	100 µAh	3 V	4.5 V	1.080 J

is a series combination of two micro-batteries. For each of the storage components, the maximum usable stored energy is listed in Table 4.2. For the supercapacitors, the maximal usable energy is calculated using (4.1). For the battery configuration, it was estimated using its data sheet. For the effective minimum and maximum voltages of each component i, the minimum input voltage of the buck converter and the discrete charge settings of the harvesting IC have to be taken into account, as shown in (4.2) and (4.3).

$$E_{usable,i} = \frac{1}{2} \cdot C \cdot (V_{max,eff,i}^2 - V_{min,eff,i}^2) \tag{4.1}$$

$$V_{min,eff,i} = max(V_{min,i}, V_{buck,min}), \text{ where } V_{buck,min} = 1.925\,\text{V} \tag{4.2}$$

$$\begin{aligned} &V_{max,eff,i} = max(\{v \in \mathbb{V}_{Harvester} \mid v \leq V_{max,i}\}), \\ &\text{where } \mathbb{V}_{Harvester} = \{2.7\,\text{V}, 3.63\,\text{V}, 4.12\,\text{V}, 4.5\,\text{V}\} \end{aligned} \tag{4.3}$$

To put these numbers into perspective, the amount of energy that can be stored in the DMT3N4R2U224M3DTA0 is sufficient to, as an example, provide an average current of 15 µA at 1.8 V for 13.5 hours, with a buck efficiency of 90% taken into account. This example shows that the main purpose of the storage element is to supply the board with enough power for short periods without harvesting, e.g. over night, but does not suffice for multiple days.

As long as the buck converter is active, it draws power from the storage component until its input voltage falls below a threshold of 1.925 V. Some types of storage components, such as the ITX121010A batteries, may not be drained below a certain voltage to prevent damage. For such components, a voltage supervisor from ROHM's BU43xx series is used to enable the buck converter only when the voltage of the storage component is above the minimum voltage of the storage component. The BU43xx series has a detection range of 0.9 V to 4.8 V in 100 mV steps and an ultra-low current consumption, which makes them well-suited for this task. For storage components like the supercapacitors, where such a supervision is not necessary, the voltage supervisor can be replaced with

a 0 Ω resistor between pads 1 and 2 of the supervisor footprint to always enable the buck converter.

As programming and debugging the platform using only the harvested energy is very unpractical, the PCB can also be powered from an external source. The pin for the external power supply has an over-voltage, reverse-voltage and over-current protection. It bypasses the harvesting and buck converter and by mounting the appropriate jumpers, it can be directly connected to power domain 0, as shown in Figure 4.3. In order to test sub-circuits of the PCB easier and allow to disconnect some parts of the circuit, the PCB has three jumpers (0 Ω Resistors), which divide the harvesting and storage part as shown in Figure 4.3. The first jumper, J2, connects the energy storage component to the input of the buck converter. If this jumper is removed, it allows the harvesting and energy storage side to be tested without any power being consumed by the buck converter. On the other side, this allows to test the buck converter and do power measurements including the buck converter losses without risking damage to the energy storage component or the harvester. The second jumper, J3, connects the output of the buck converter to power domain 0. This jumper has to be removed when external power is applied to the circuit, as the external power would interfere with the buck converter. The last jumper, J4, connects the external supply to power domain 0. This jumper can be removed to disconnect the protection circuit of the external supply from power domain 0, and thus reduce the current leakage of the board.

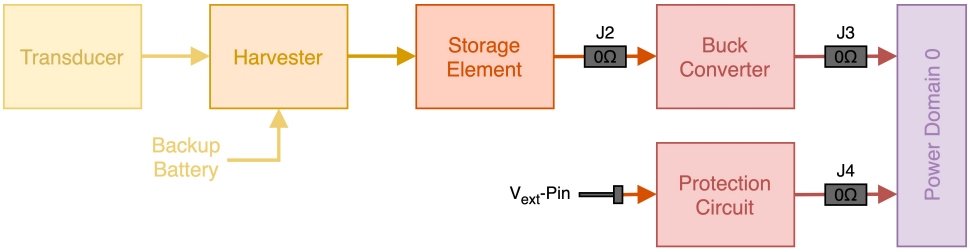

Figure 4.3: Division of Energy Supply using Jumpers

4.2 Wireless Communication

The implementation of the communication processor and BOLT are largely based on the *DPP2 LoRa ComBoard*[5] developed at TEC. The main components of the subsystem are the communication processor, which is implemented on an STM32L431, and BOLT, which is implemented on an MSP430FR. Additionally, the SX1262 is used as a LoRa transceiver. The biggest change compared to the *DPP2 LoRa ComBoard* is the new chip antenna, which replaces the SMA connector and whip antenna. This change was required to keep the size of the PCB

small, but it reduces the performance of the antenna. The software implementation of these systems is not part of this project, instead the existing BOLT[1] and Flora[4] libraries are used on the BOLT and communication processors, respectively.

4.3 Environmental Sensing

To implement the requirements for the environmental sensing described in Section 3.3, five sensors were chosen:

- VEML7700: A high-accuracy ambient light sensor manufactured by Vishay Semiconductors. This sensor can be used to track the lighting conditions of the board. Its placement next to the solar panel is chosen to make sure the data collected from the sensor best reflects the light intensity on the solar panel. Its position is indicated with a '1' in Figure 4.4.
- LIS3DH: STMicroelectronics' 3-axis accelerometer, which can be used to detect the orientation and movement of the board. It is placed on the back side of the PCB, as it does not require direct access to the environment. Its position is indicated with a '2' in Figure 4.5.
- SHTC3: A humidity and temperature sensor manufactured by Sensirion. It provides the fundamental environmental conditions the board is operated in. This data is also important for the data collected by the other sensors, especially the SGP40. To prevent incorrect temperature measurements of the sensor caused by direct light irradiation, the sensor is placed on the back side of the PCB. However, to increase the accuracy of the humidity measurement, the sensor requires as much air flow as possible. For this, the sensor was placed on the edge of the PCB, indicated with a '3' in Figure 4.5.
- SCD41: Sensirion's high-accuracy CO_2 sensor with temperature and humidity compensation. With this sensor, the CO_2 concentration of the air in a room can be monitored. It is placed on the top side of the PCB to achieve maximum air flow, indicated with a '4' in Figure 4.4.
- SGP40: An indoor air quality sensor by Sensirion, which measures the VOC concentration and converts it into a reference index. The VOC index is an important metric for air quality. It is also located on the top side for better air flow and its position is indicated with a '5' in Figure 4.4.

Combined, the first two sensors provide useful data for the harvesting conditions, and the latter three of these sensors provide a wide range of indicators

[1] https://github.com/ETHZ-TEC/BOLT

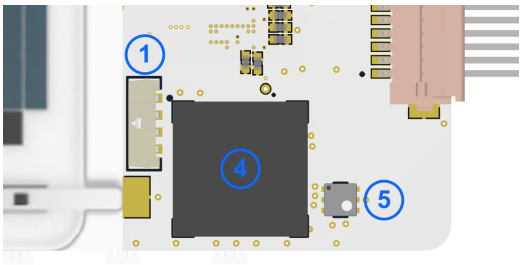

Figure 4.4: Sensors located on the Top Side

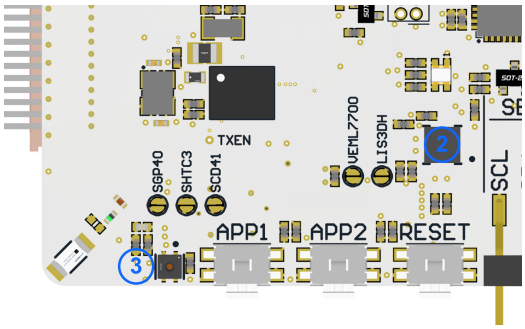

Figure 4.5: Sensors located on the Bottom Side

for air and environment quality. Additionally, the accelerometer can be used as a user input.

All sensors have a digital Inter-Integrated Circuit (I^2C) interface and are connected to a common I^2C bus, which is controlled by the application processor. Additionally, there is also a pin header with the I^2C signals, which allows to debug the sensors on the board, or connect additional external sensors. All of these sensors reside in power domain 1 and can thus simultaneously be powered on and off by the application processor. To more selectively control which sensors are powered and to allow more precise power measurements, each of the sensors has an individual solder jumper to disconnect its power input pin from power domain 1. These solder jumpers can also clearly be seen in Figure 4.5.

The sensors were selected with great care to keep the quiescent and idle currents as low as possible. In pursuit of this primary target, some of the secondary design objectives of the board could not be fulfilled. As such, two of the sensors cannot be operated with the minimum circuit voltage of 1.8 V: The VEML7700 and the SCD41 require a minimal voltage of 2.5 V and 2.4 V, respectively. Also, the SCD41 has a height of 6.5 mm, which is considerably taller than the other components of the PCB.

4.4 Application Processor

The application processor is the central component of the whole platform. For this, Ambiq Micros' Apollo3 Blue Plus MCU was selected. It features an ARM Cortex M4 Core with an integrated Floating Point Unit (FPU) and it can run with a core clock frequency of up to 96 MHz. One of the main reasons for choosing this MCU is its low deep sleep current and particularly its unrivaled run current of just 6 µA/MHz, as will be further detailed in Section 4.5. In Chapter 3, the main responsibilities of the application processor were described. The design implementation of these different task is described below.

4.4.1 Energy Storage Measurements

The state of the energy storage component is measured in three different ways. The first - and straight forward - method is measuring the voltage of the energy storage component. The harvester can charge the storage component to up to 4.5 V, but this voltage is higher than the maximum analog input voltage of the Apollo, which is limited to the internal voltage reference of 2.0 V. Thus, a voltage divider with a ratio of $\frac{4}{9}$ is used to convert the 0...4.5 V range of the storage component into a range of 0...2 V for the Analog to Digital Converter (ADC) reference. To prevent leakage currents through the resistors, the voltage divider is gated using a high-side power switch. The SIP32431DR3, which was chosen for this task, reduces the input leakage far below 1 nA across the whole measurement rage according to its data sheet. After the voltage divider, a capacitor is added to low-pass filter the measurement before the ADC and prevent measurement inaccuracies caused by the ADC input leakage currents. With a cut-off frequency of 459 Hz, the switching noise of the harvester and buck converter can be suppressed. However, this introduces the disadvantage that the switch has to be closed for 1.6 ms to charge the capacitor to 99% and allow for an accurate measurement. The full measurement circuit is shown in Figure 4.6.

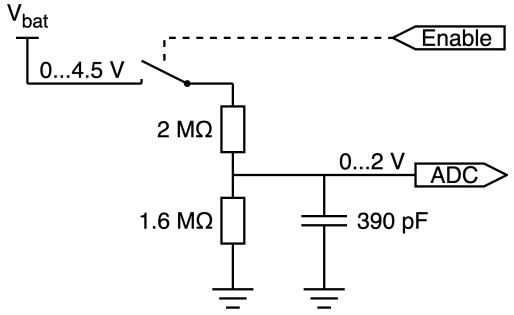

Figure 4.6: Storage Element Measurement Circuit

In addition to the continuous voltage measurement, the PCB also features a

voltage supervisor to detect if the storage component is above a certain threshold and can be used to indicate if the storage component is full or sufficient energy for a certain task is available, depending on the application and storage component. The TLV840 series from TI, which was selected for this, has components with threshold voltages in the range of 0.8...5.4 V in 100 mV steps. The default component has a threshold value of 4.0 V, which offers a good trade-off for all three default energy storage components.

The third and last indicator for the charge level of the storage element is the power good signal of the buck converter. This signal is pulled low by the buck converter if it can not regulate its output to the selected voltage. It can serve as an indicator to the application processor that the charge state of the storage component is too low and the buck converter can no longer supply the demand of the power domains before the power is completely cut off.

4.4.2 Power Distribution Control

The application processor can enable and disable the power domains 1 and 2 to reduce the leakage current when necessary. As the power domains 1 and 2 have the same operating voltage level as power domain 0, they can each be gated to power domain 0 using a P-channel Metal–Oxide–Semiconductor Field-Fffect Transistor (PMOS). Both of these PMOS are controlled by the application processor using inverted logic. To guarantee a defined state of the power domain, the control signals each have a pull resistor. The pull resistor is either pull-up to have the power domain normally-off, or pull-down to have it normally-on. However, the use of these pull resistors also introduces a leakage current when the application processor pulls the control signal opposite to its normal state.

4.4.3 Sensor Readout

The environmental sensors described in Section 4.3 are connected to a common I^2C bus, which is controlled by the application processor. The pull-up resistors of the I^2C bus are connected to the same power domain as the sensors to prevent power leakage via the I^2C lines when power domain 1 is disabled. To further reduce the power leakage, the Apollo pins used for the I^2C communication are put into a high impedance state when power domain 1 is disabled.

4.4.4 Communication with Communication Processor

The application processor communicates with the communication processor via BOLT. For this, the application processor implements the SPI and control signals, as described in [3]. Additionally, the application processor can also read

the indicator signal for the communication processor to check whether the communication processor has already read all messages from BOLT.

4.4.5 User Feedback

Displays

The board features two electrochromic segment displays, which are used as the primary way for the Application processor to provide feedback to the user. Each segment of the display can individually be colored by applying a positive voltage to the segment, or bleached by applying a negative voltage. The electrochromic displays have the property that they keep their state for several minutes, even if no power is provided to them anymore. An example of this retention can be seen in Figure 4.7. This property makes them well-suited for low-power applications. However, they have the down side that they have to be periodically refreshed. The board has a fixed fill-bar display with 7 segments, and a connector where optionally another display can be inserted. The largest display that can be inserted into this connector is a signed 2-digit display. The fill-bar and the signed 2-digit display can be seen in Figure 4.1a. The usage of the displays depends on the application. For example, the fill-bar can be used to indicate the charge state of the storage element, or the air quality and the signed 2-digit display can show the humidity or temperature. The software library for this platform comes with a custom driver for the displays, which was developed as part of this project. This stateful driver provides a simple interface to display numbers and fill levels on the displays and takes care of updating and refreshing the displays when needed.

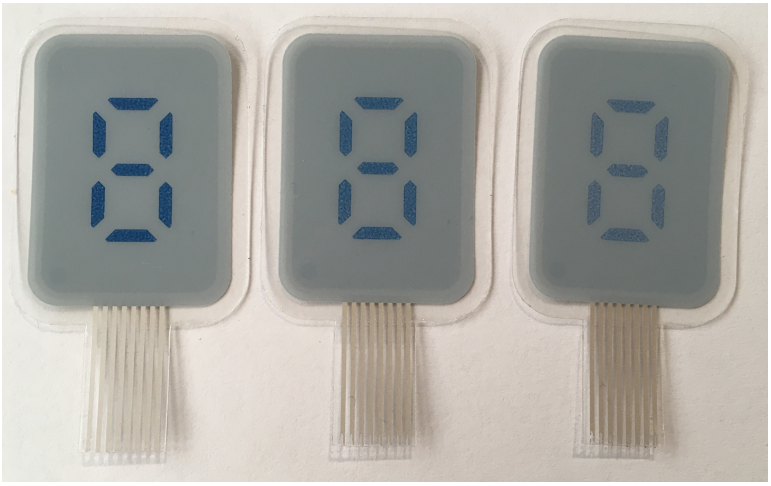

Figure 4.7: Fade-out of Electrochromic Display: freshly polarized (left), 15 minutes after polarization (center) and 30 minutes after polarization (right)

Bluetooth Communication

As an additional way to provide user feedback, the Apollo3 Blue Plus MCU also has an integrated BLE module, which can be used as a wireless method to provide the user with data from the platform, and allow the user to interact with the board. The application uses the full Bluetooth stack implemented by the ARM Cordio-B50 library. The PCB has a chip antenna to send and receive data.

Debugging

The PCB also has various features to simplify application development and debugging on the board. The PCB has two user buttons, three Light-Emitting Diodes (LEDs), two General-Purpose Input/Output (GPIO) pins and a pair of Universal asynchronous receiver-transmitter (UART) pins. The GPIO and UART signals are available on one of the pinheaders. All of them are located in the bottom center on the back side of the PCB. To make application development easier, a Board Support Package (BSP) for the PCB was created. This BSP contains the necessary pin definitions for all peripherals and provides functions for basic operations of the board, like enabling and disabling power domains.

4.5 Current Consumption

The goal of the platform is to be ultra-low-power as it is powered only by harvesting. For this, the typical quiescent and operating currents of the different systems are of utmost importance. Table 4.3 summarizes the current drains under various conditions. Unless otherwise noted, the data in this table is taken from or calculated using the datasheets of the respective components. To keep the table brief, leakages below 10 nA, for example caused by signal inputs or protection diodes, are not listed.

The quiescent current value of the Apollo assumes deep sleep with 8 kByte Static Random-Access Memory (SRAM) retention. This parameter is from the datasheet rev. 1.0.0 and was removed in revision 1.1.0, and may thus not be a reliable parameter. The active current assumes code execution from internal flash memory with caching enabled, 48 MHz core frequency, all peripherals disabled and only 8 kB SRAM used. The expected current consumption for the BOLT + LoRa system are taken from measurements on the DPP2 LoRa ComBoard[5, page 31]. The values listed in Table 4.3, especially the active current consumptions, may widely differ from the theoretical values under real-world conditions, however, they are still listed here to provide a rough overview of the systems' current consumption.

Table 4.3: Theoretical Current Consumption of Components and Systems

Component/System	I_Q	I_{act}	Source	Active Condition
DMT (Supercap.)	2 µA	2 µA	V_{BAT}	Always
GA209F (Supercap.)	1 µA	1 µA	V_{BAT}	Always
BU4322G (Supervisor)	0.25 µA	0.4 µA	V_{BAT}	Buck enabled
TLV840 (Supervisor)	0.15 µA	0.15 µA	V_{BAT}	Always
TPS62740 (Buck)	0.07 µA	0.46 µA	V_{BAT}	Buck enabled
Cap voltage meas.	0 µA	1.0 µA	V_{BAT}	measurement active
Apollo3 Blue Plus	1.6 µA	672 µA	PD0	MCU Core active
Apollo3 BLE Module	0 µA	3000 µA	PD0	BLE transmission
Signed 2-digit display	0.024 µA	500 µA	PD0	Display updated in 1 s
Fill-bar display	0.012 µA	533 µA	PD0	Display updated in 1 s
Cap Full signal	0.01 µA	0.9 µA	PD0	Cap not full
Cap voltage meas.	0 µA	0.9 µA	PD0	measurement active
PD1 Enable	0 µA	0.9 µA	PD0	Sig. opposite to pull
PD2 Enable	0 µA	0.9 µA	PD0	Sig. opposite to pull
V_{EXT} Protection	0 µA	0.075 µA	PD0	J4 soldered
SCD41	150 µA	3200 µA	PD1	Low-power meas.
SGP40	34 µA	3500 µA	PD1	measurement
LIS3DH	0.5 µA	6 µA	PD1	50 Hz low power mode
VEML7700	0.5 µA	2 µA	PD1	Lowest power mode
SHTC3	0.3 µA	270 µA	PD1	Low-power meas.
BOLT + LoRa System	1.7 µA	∼6 mA	PD2	Idle
		∼12 mA	PD2	Radio in Rx Mode
		<150 mA	PD2	Radio in Tx Mode

The SCD41 is very power-hungry compared to the other sensors. According to the datasheet, a single measurement typically consumes 243 mJ, which is a large fraction of the energy that can be stored on the board (see Table 4.2). Even under good lighting conditions, the solar panel requires about 15 to 20 minutes to collect this amount of energy. While the SGP40 has a similar active current as the SCD41, its measurement time is much lower and thus the energy consumption is much smaller. With the duty-cycling technique described in [9], the average consumption of the sensor can be reduced to prevent the quiescent current of the SCD41 from draining the energy storage component.

4.6 Operating Modes

The board has many different subsystems, which can be activated and deactivated individually. These functionalities are grouped together into three basic operation modes, which are ordered by increasing power consumption:

- Operation Mode 1 - Sensors + Display: This mode has the lowest power consumption of all modes. The application processor periodically samples the sensors on the board and displays the sensor data on the electrochromic displays. Power domain 1 is only enabled for the brief time required to retrieve the sensor readouts. Power domain 2 is always switched off and therefore no data can be transmitted or received.
- Operation Mode 2 - Sensors + Display + BLE: This mode works in the same way as operation mode 1, but additionally, the sensor data is also sent via Bluetooth.
- Operation Mode 3 - Sensors + Display + BLE + LoRa: This mode includes everything from operation mode 2, and additionally the LoRa communication is also activated. This allows the data to be sent over longer distances, but it is also the mode with the highest power consumption.

When the board is not actively doing something, it is put in deep sleep until the next sensor measurement is started or communication occurs. In this mode, everything that can be disabled is turned off to reach the lowest possible current consumption. The current consumption in this mode, seen from the perspective of the buck converter output, is 1.65 µA.

Chapter 5

Results

This chapter covers the testing of the platform, the results that were obtained during the testing, and the discussion of these results. In a first step a prototype PCB was manufactured and assembled. The subsystems of the PCB were individually tested, as shown in the first section of this chapter. With the assembled and tested prototype, current measurements were performed to obtain the power consumption of the board in the different operation modes. The results from these measurements are listed and discussed in the second section of this chapter.

5.1 PCB Assembly and Testing

The design shown in the implementation chapter was manufactured and then assembled. For the assembly, first the components on the bottom of the PCB were populated by hand and soldered using the reflow process, with the exception of the components not compatible with this process. These components were soldered by hand in a second step, together with all passive components on the top side of the PCB. The solar panel and displays were not mounted in this step. Additionally, the jumpers on the bottom side discussed in Section 4.1 were also not populated yet, to allow for smaller parts of the circuitry to be tested individually. The bottom side of the assembled PCB can be seen in Figure 5.1.

The PCB prototype, which was also used to obtain all the measurements in the next section, was populated with the following configuration:

- Buck Converter Output Voltage: 1.8 V.
- MPPT: 85%.
- Harvester Configuration: 7 (Charge storage to 4.12 V).
- Primary battery usage: None.

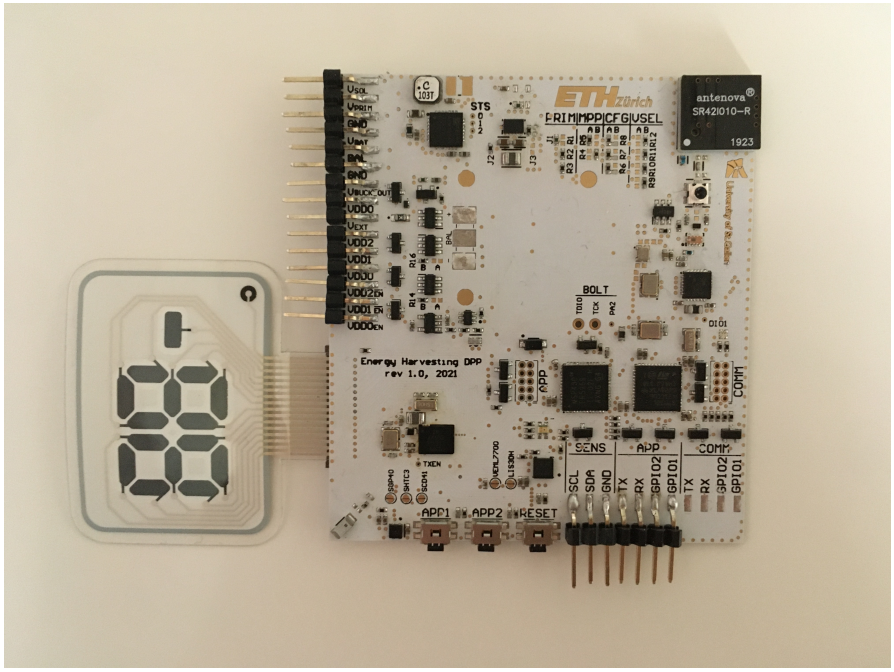

Figure 5.1: Bottom Side of the Assembled PCB

- Energy Storage Component: DMT3N4R2U224M3DTA0.
- Power Domain 1: Normally On.
- Power Domain 2: Normally On.
- Mounted Sensors: SHTC3, LIS3DH. Supply jumpers open.

In a first step, the harvesting circuit was tested by illuminating an externally connected solar panel and measuring the voltage level of the storage element. Additionally, the status pins of the harvester were measured and validated. This shows the basic functionality of the harvesting and energy storage circuit. In the second step, with jumper J2 added, the functionality of the buck converter was verified and the status signal of the buck converter, as well as the other signals for the energy storage measurements were checked and validated.

Next, power domain 0 was tested. In this test, it was discovered that not all pads of the Apollo3 made contact with the PCB on the prototype board. As one of the unconnected pins was the supply pin for the core and memory power domains of the MCU, the Apollo3 was not able to start up. These soldering issues were partially fixed by an additional soldering round in the reflow-oven. With this fix most, but not all, of the soldering issues could be resolved. The pins which are still not connected are the SCL signal of the I^2C-bus for the sensors, two segments of the signed 2-digit display, and some of the debug pins

like LEDs and buttons. While the debugging pins and the unconnected display segments are not severe for a prototype PCB, the unconnected I^2C signal makes it impossible to test the sensor communication on the board.

In order to circumvent the soldering issues, all software drivers for the components on the PCB were tested on the evaluation board of the Apollo3 Blue Plus, using break-out boards for all the peripherals. An example of this can be seen in Figure 5.2, where the SHTC3 sensor driver is tested and the humidity value is shown on the electrochromic display. Additionally, due to the time lost by the soldering issues, it was not possible to test the components for the communication processor within the time frame of this project.

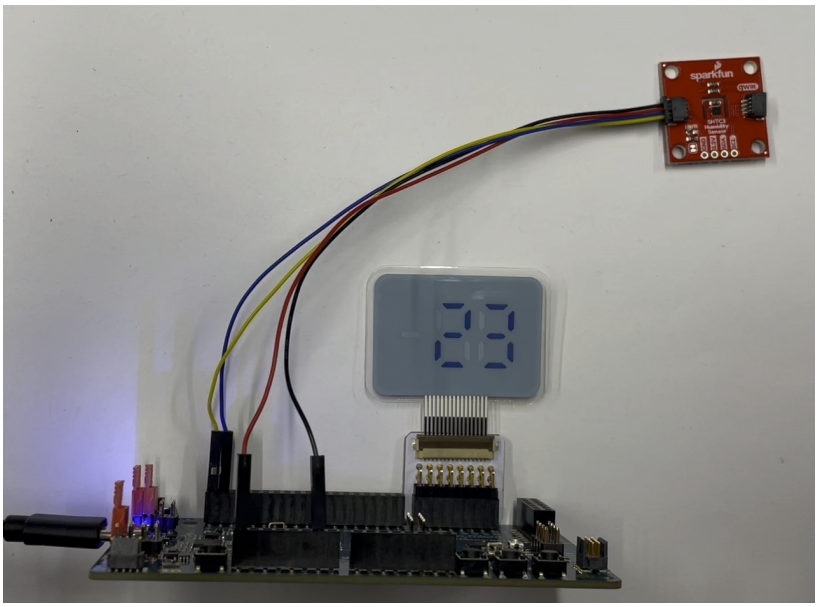

Figure 5.2: Software Testing on the Apollo3 Evaluation Board

5.2 Power Consumption

The platform is designed to use energy harvesting and should thus be ultra-low-power. Consequentially, the power consumption is the most important characteristic of the board and must be measured. Due to the soldering issues of the application processor, it was not possible to measure the power consumption of all the operation modes this PCB was designed for. Instead, the measurements were focused on the parts of the board for which basic functionality was verified. The current consumption for three modes were measured: Apollo deep sleep, Apollo + Display and Apollo + BLE. This section first explains the measurement setup, then shows the results of the measurements and finally discusses the results.

5.2.1 Measurement Setup

The power consumption of the board is measured by supplying power through the external supply pin, which bypasses the harvesting part and the buck converter of the board. Thus, the power measurements provided in this section do not include the losses of the buck converter, the leakage of the storage element, etc. All measurements were performed with an *Otii Arc*, which acts both as voltage supply and current measurement device. The supply voltage for the PCB is set to 1.95 V. This voltage is higher than the normal operating voltage of 1.8 V, as the voltage drop over the ammeter can result in brown-out events of the microcontrollers whenever sudden current spikes occur.

In order to improve the power measurements, the jumper connecting the output of the buck converter to Power Domain 0 and the pull-up resistor of the Bucks' power good signal were removed to prevent reverse leakage through the buck converter, which tries to actively discharge its output when it is not enabled. Further, the solar panel and the storage element were disconnected to prevent any damage to the harvesting circuitry during the measurements.

For all the tests, power domains 1 and 2 are disabled by software, and all unused GPIO pins of the Application processor are in a high impedance state or pulled low to reduce the energy consumption.

5.2.2 Apollo Deep Sleep

This measurement is intended to show the lowest possible current consumption of the board and allow for comparison with the theoretical value from Section 4.5. For this, the Apollo is put into deep sleep mode 2 with 32 kByte SRAM retention. This is the lowest power mode that still allows to preserve some minimal software state. The average current consumption was measured to be 8.21 µA when in deep sleep mode, resulting in a power consumption of 16.0 µW.

5.2.3 Apollo + Display

This measurement is used to characterize the current consumption of the display and its software driver, using the signed 2-digit display. The display shows a counter, which is increased by one every 60 Seconds. The bleaching and coloring time are each set to 500 ms, thus it takes 1 s to update the value shown on the display. The current trace was recorded over a duration of 10 Minutes. With these parameters, an average current consumption of 17.5 µA was recorded, with peaks up to 2.4 mA. During the phases where the display is not being updated and the Apollo is in deep sleep, the average current consumption is 8.95 µA. During the display update, the average current consumption is 522 µA.

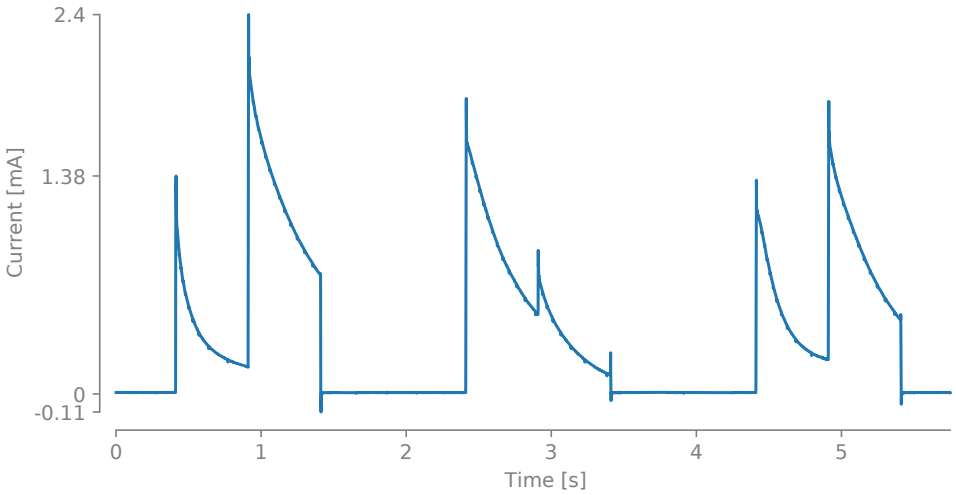

Figure 5.3: Display Current Consumption

Figure 5.3 shows the current trace when the display value is updated every 2 seconds. In this current trace, the display is updated three times. In the first update, the value is set to 00, in the second update it is set to 01, and in the third it is set to 02. This example clearly shows that the current consumption of the display strongly depends on the difference between the previous value and the new value. To display 00, a lot of segments need to be colored an thus the second half of the first display update has a higher current consumption than the first half. The current trace also shows peaks in the beginning, middle and end of each update phase, which indicate when the Apollo is running.

5.2.4 Apollo + BLE

The third measurement shows the current consumption of the Apollo with periodic BLE transmissions. The application software is based on a Real-Time Operating System (RTOS), with the BLE communication implemented as a task. For this measurement, the Apollo sends a BLE advertisement every 5 seconds. Over a duration of 5 minutes, the resulting average current consumption is 18.6 µA. The median BLE transmission causes a current peak of 4.63 mA, with a few outliers peaks of 7.57 mA. During deep sleep, the average current consumption is 13.7 µA. Figure 5.4 shows a 30 seconds segment of the current trace with 6 BLE transmissions. Additionally, three wake-ups caused by the RTOS can be seen.

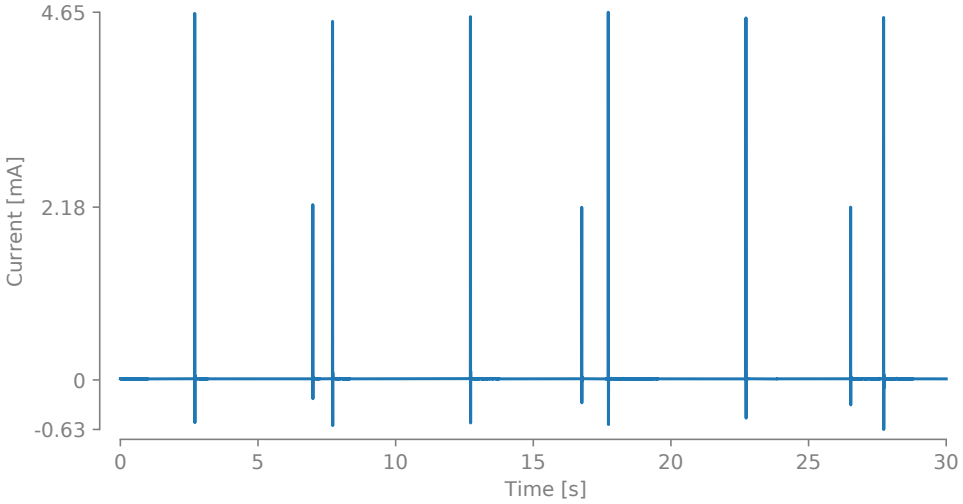

Figure 5.4: BLE Current Consumption

5.2.5 Summary

The results of the current measurements are summarized in Table 5.1. It can clearly be seen that both the average current as well as the consumption in deep sleep phases increase with respect to the constant deep sleep when additional systems of the PCB are active.

Table 5.1: Current Consumption Measurements

Active Systems	I_{avg}	I_{deep_sleep}	I_{peak}	Wake-up period	Energy Autonomy
Apollo3	8.21 µA	8.21 µA	-	N/A	24.7 h
Apollo3 + Display	17.5 µA	8.95 µA	2.4 mA	60 s	11.6 h
Apollo3 + BLE	18.6 µA	13.7 µA	4.64 mA	5 s	10.9 h

The last column in Table 5.1 shows the theoretical energy autonomy for all three active system cases. These values show the duration the system can remain active only using the energy available in the energy storage component, without any new energy being provided by the harvesting. The calculation assumes an initially full DMT3N4R2U224M3DTA0 (1.46 J), an operating voltage of 1.8 V, a buck converter efficiency of 90 % and the average current consumption value in the respective I_{avg} entry.

5.2.6 Discussion

Quiescent Current Consumption

The current consumption from the deep sleep measurement shows the quiescent current consumption of the PCB. It is clearly higher than the theoretical value of 1.65 µA, which is the sum of all quiescent currents in power domain 0 from Table 4.3. A part of this difference can be explained by leakages trough pull resistors. On the prototype PCB, both power domains are configured as normally-on. However, in deep sleep these power domains are off and thus the pull resistors are conducting current. Additionally, as the energy storage component was removed, the signal indicating if the storage element is full is also pulled low and thus there is an additional pull resistor conduction current. Each of these three resistors has a value of 2 MΩ, resulting in a combined leakage of 2.93 µA. Thus, with a better configuration and more ideal operating conditions, these leakages are not present and a deep sleep current consumption down to 5.28 µA is possible. The remaining difference of 3.63 µA to the theoretical value of 1.65 µA cannot be explained with certainty, but it is possible that more hardware settings on the Apollo3 could be made to further reduce its current consumption.

Deep Sleep Consumption Comparison

The slight increase of the deep sleep current consumption when the display is active with respect to deep sleep only can be explained by the active timer and increased retained memory required by the display driver. This difference is even larger for the Apollo3 + BLE case, but it can be explained with the same reasoning. The Apollo3 + BLE mode runs with an RTOS and BLE stack, which both require additional active memory and peripherals. In fact, the RTOS configuration used in this implementation keeps all memory active, which explains the large increase in current consumption.

Active Current Consumption

As mentioned in Section 5.2.3, the average active current during display updates is 522 µA. This value is close to the expected active current of 500 µA from Table 4.3 (neglecting the Apollo3 deep sleep current).
The peak current consumption for the BLE example is close to what was expected in Table 4.3. The measured peak value of 4.64 mA is only slightly above the expected average active current of 3.67 mA (0.67 mA Apollo3 active current and 3.0 mA BLE transmission).

Energy Autonomy

The calculated energy autonomy durations for the two active examples Apollo3 + Display and Apollo3 + BLE are almost half a day and thus show that the system can sustain operation during short night periods where not enough light is available for harvesting. With the resistor configuration improvements mentioned in the discussion of the quiescent current, the energy autonomy could in theory even be extended beyond 12 hours for both examples.

Chapter 6

Conclusion and Future Work

6.1 Conclusion

In this project, a harvesting based platform for indoor environmental sensing was developed. With the combination of a solar panel and a short-time energy storage component, the platform can be operated energy-independent. Its different operating modes allow the energy consumption to be adapted depending on the available energy, and in its lowest operating mode, it can resume operation even over short night periods where no energy can be harvested. The on-board sensors of the PCB make it possible to collect data about temperature, humidity and air quality in a room, as well as the lighting conditions of the board. The collected data can be directly shown to the user using the low-power displays, or it can be transmitted to the user via BLE. In addition to the short-range BLE communication, the board can also communicate over long links using LoRa. This also allows the collected data to be stored off-board.

A prototype PCB was assembled and the basic functionality of the design was verified. Additionally, power measurements were conducted, and most are very close to the expected consumption values.

6.2 Future Work

The design and prototype developed in this project serves as a foundation for various projects in different research directions. However, due to the soldering issues mentioned in Section 5.1, and the resulting loss of time, some parts of the testing and profiling are not done yet. For the harvesting subsystem, measurements regarding efficiency of the harvesting and the leakage current of the storage element and its surrounding components can be done. For the sensors, testing their performance and power consumption on the PCB remains to be done. The BLE communication functionally works, but more work can be invested to tune the impedance matching and measuring the transmit power of

the board. The communication processor with LoRa and radio communication also remains to be tested, impedance matched and profiled.

According to the theoretical values, the power consumption of the Apollo3 in deep sleep is higher than it should be. More work in this direction could be done to reduce the deep sleep power consumption and thus increase the energy autonomy of the board. Also, the current implementation of the RTOS leaves room for improvements, as it currently does not deactivate unused memory in deep sleep at this time.

With the combination of energy harvesting and synchronous communication capabilities, it is also possible to develop and test energy aware synchronous communication protocols on this platform. This includes research on how a node decides if it can send data with its available energy, as well as how the network handles it if a node cannot participate in communication because it does not have enough energy available.

As the Apollo3 Blue Plus can execute TensorFlow Lite models, it is possible to improve the collected sensor data using on-board machine leaning. It was demonstrated in [9] that some types of sensors can be duty-cycled and the resulting loss in sensitivity can be compensated using predictive sending. Further work in this direction can be used to improve the accuracy of the collected gas sensor data and reduce the power consumption of the board.

PCB Schematics and Layout

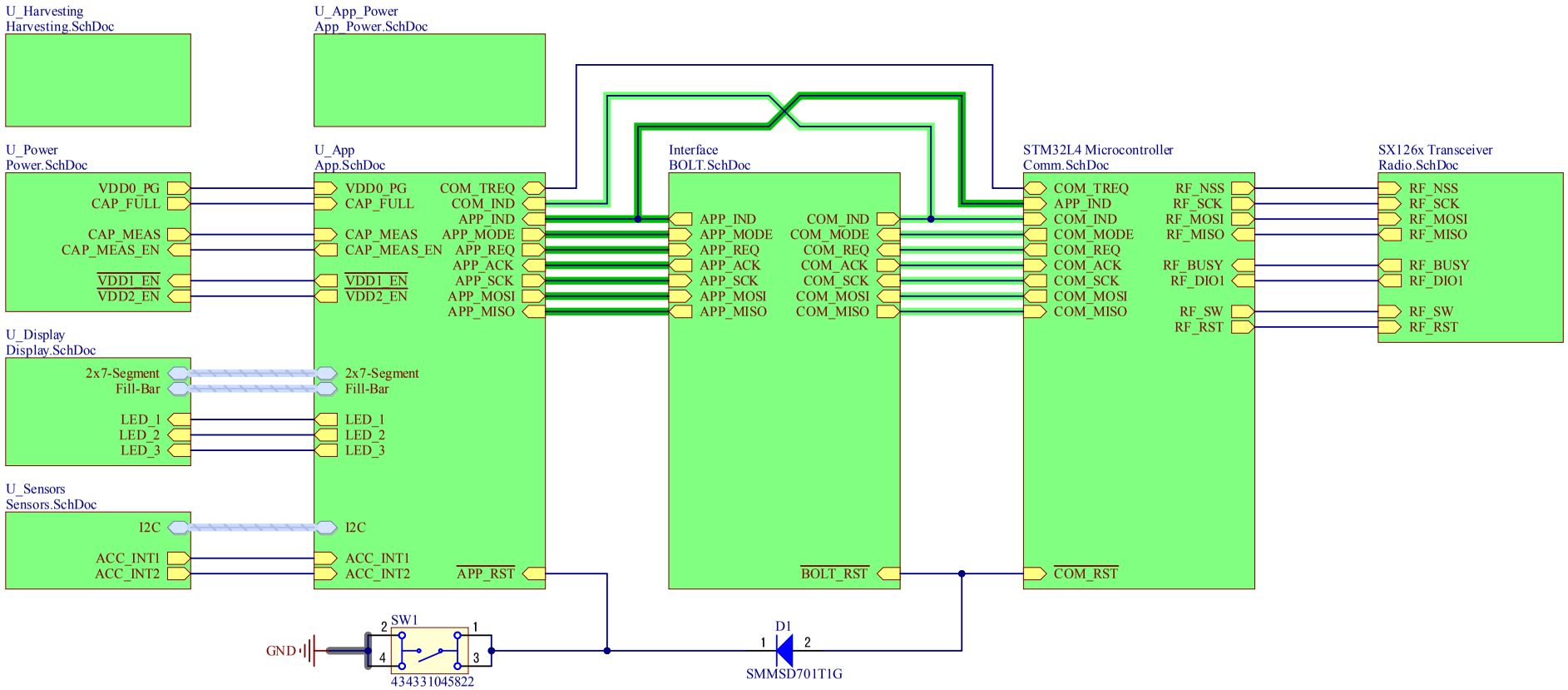

ETHZurich

Logo ETH Zurich

University of St.Gallen
Institute of Computer Science

ETH

Eidgenössische Technische Hochschule Zürich
Swiss Federal Institute of Technology Zurich

Project:

Harvesting Based DPP Overview

Drawing number: 1	Rev: 1	Format: A4 Q	Laboratory: Computer Engineering Group, TIK	Sheet: Overview.SchDoc	
Date: 12/9/2021 1:15:06 PM			Drawn by: Luca Rufer	Page 1	of 10
File: Y:\EharvDPP_PCB\Overview.SchDoc					

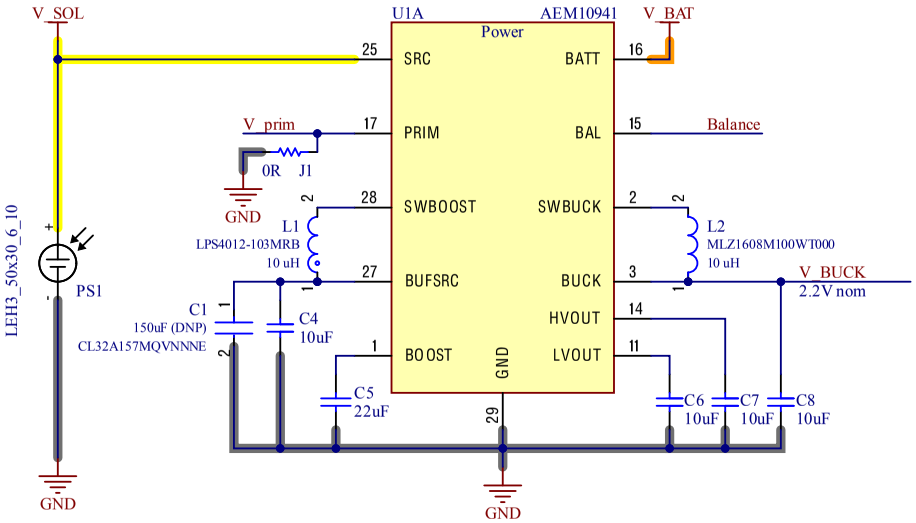

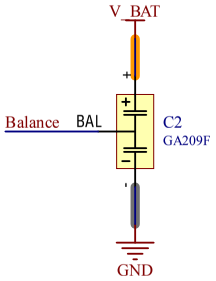

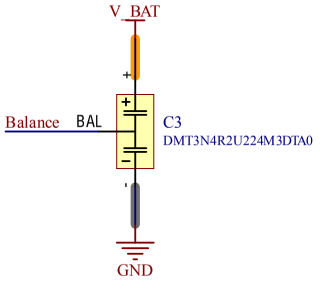

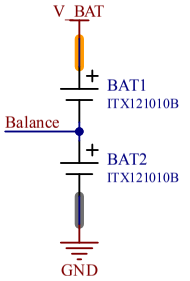

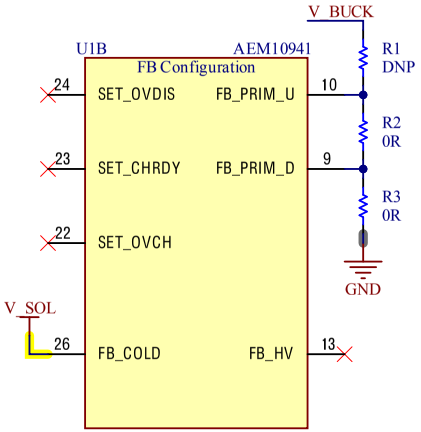

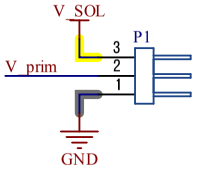

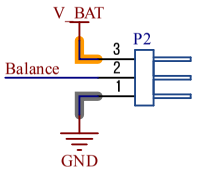

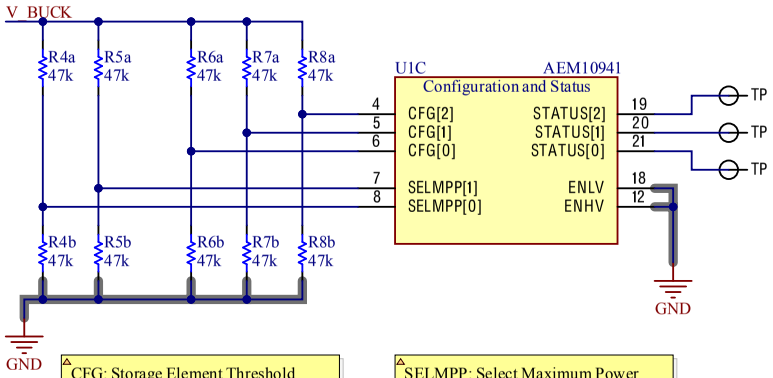

When using no primary Battery:
do not mount: C1, R1
mount J1, R2 and R3 as 0-Ohm Resistors, C4 with 10uF

When using a primary Battery:
do not mount: J1, R3 and C4.
mount C1 (150uF), R1 and R2 as stated in the AEM Datasheet.

Pull Balance Pin to GND when not using a double layer supercapacitor. This can be done by placing a 0 Ohm resistor instead of BAT2.

CFG: Storage Element Threshold Voltages
[2] [1] [0]
0 1 1 Supercap setting 1
0 1 0 Supercap setting 2
0 0 0 Custom Setting
Set custom setting on SET_xxx Pins with voltage divider chain, or leave floating if not used

SELMPP: Select Maximum Power Point Tracking Treshold
[1] [0]
1 1 90%
1 0 85%
0 1 75%
0 0 70%
The Solar Panel has a MMP between 80% and 85%.

ETH

Eidgenössische Technische Hochschule Zürich
Swiss Federal Institute of Technology Zurich

Project: Harvesting and Energy Storage

Drawing number: 2	Rev: 1	Format: A4 Q	Laboratory: Computer Engineering Group, TIK	Sheet: Harvesting.SchDoc	
Date: 12/9/2021 1:15:06 PM			Drawn by: Luca Rufer	Page 2	of 10
File: Y:\EharvDPP_PCB\Harvesting.SchDoc					

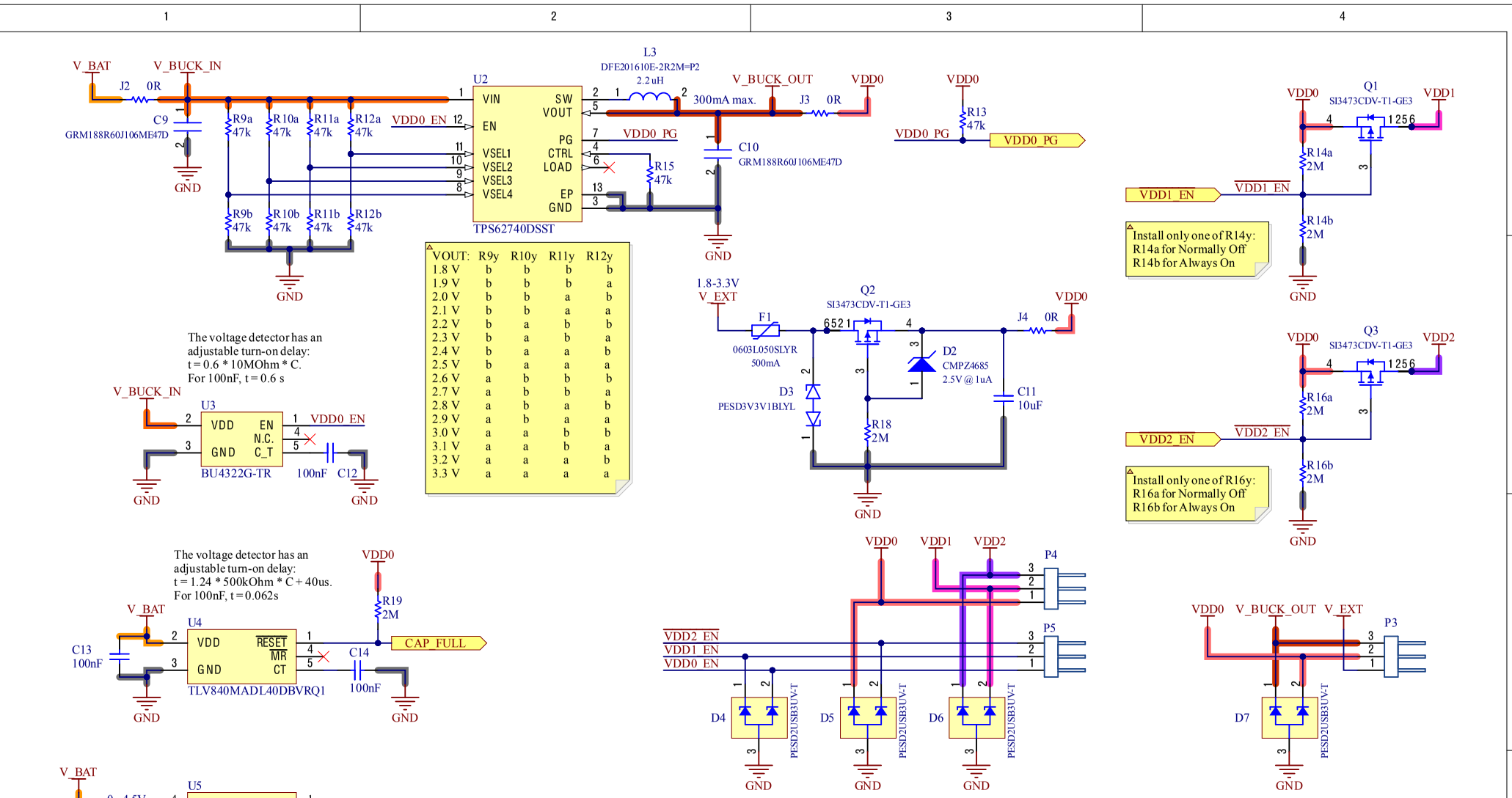

ETH Eidgenössische Technische Hochschule Zürich Swiss Federal Institute of Technology Zurich			Project: Power		
Drawing number: 3	Rev: 1	Format: A4 Q	Laboratory: Computer Engineering Group, TIK	Sheet: Power.SchDoc	
Date: 12/9/2021 1:15:06 PM			Drawn by: Luca Rufer	Page 3 of 10	
File: Y:\EharvDPP_PCB\Power.SchDoc					

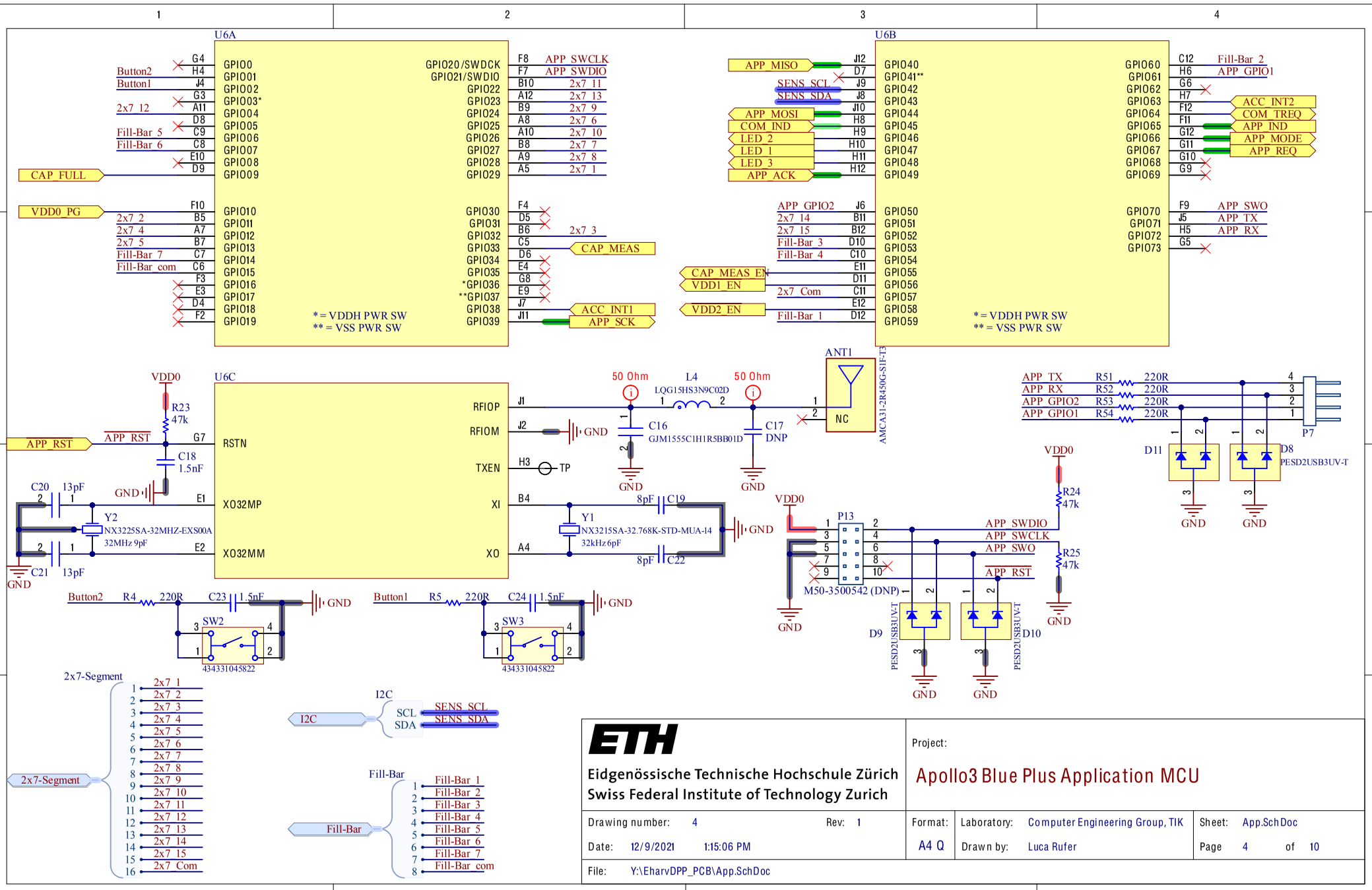
U6A
U6B
U6C
* = VDDH PWR SW
** = VSS PWR SW
ANT1
AMCA31-2R450G-SIF-T3
NC
L4
LQG15HS3N9C02D
50 Ohm
C16
GJM1555C1H1R5BB01D
C17
DNP
Y1
NX3215SA-32.768K-STD-MUA-I4
32kHz 6pF
Y2
NX3225SA-32MHZ-EXS00A
32MHz 9pF
P13
M50-3500542 (DNP)
P7
D8
PESD2USB3UV-T
D9
D10
D11
SW2
SW3
434331045822
2x7-Segment
I2C
Fill-Bar
Eidgenössische Technische Hochschule Zürich
Swiss Federal Institute of Technology Zurich
Project:
Apollo3 Blue Plus Application MCU
Drawing number: 4
Rev: 1
Date: 12/9/2021 1:15:06 PM
Format: A4 Q
Laboratory: Computer Engineering Group, TIK
Drawn by: Luca Rufer
Sheet: App.SchDoc
Page 4 of 10
File: Y:\EharvDPP_PCB\App.SchDoc

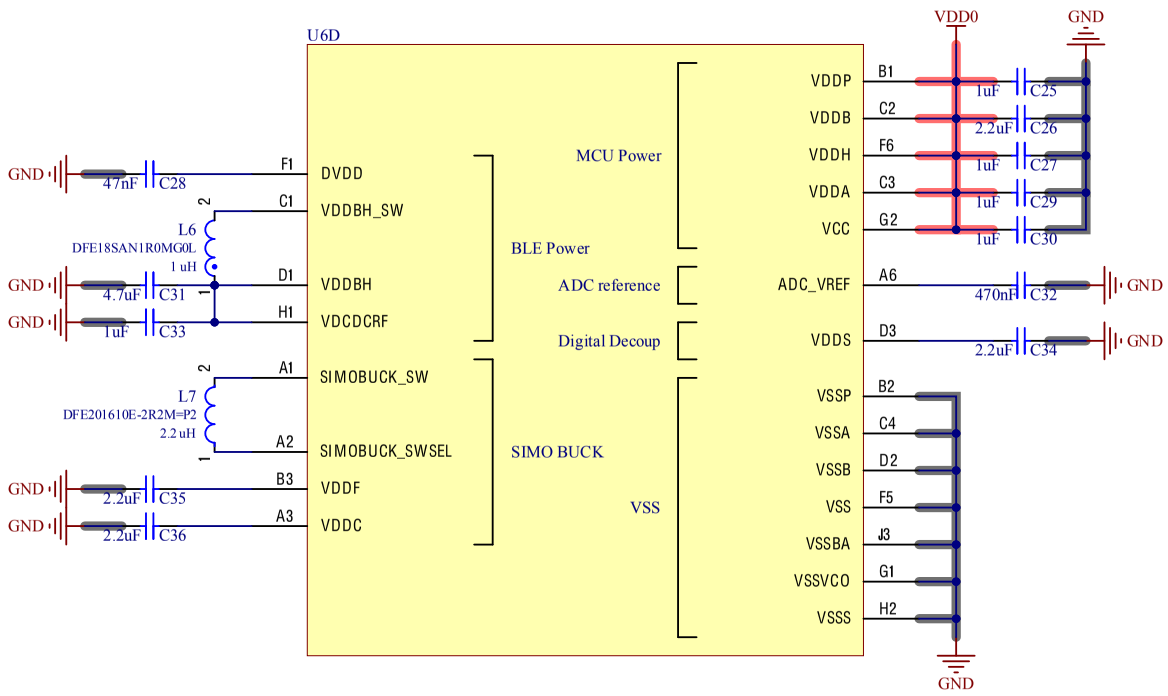

Notes on Power pins:

=== Pins with VDD connection ===
VDDP: VDD Supply for SIMO Buck Converter (also called Pad Supply)
VDDB: VDD Supply for BLE/Burst Buck Converter (generates VDDBH via external Inductor)
VDDH: VDD Supply for I/O Pads, Source for Pad 3 HS power switch and GPIO pull-ups (except Pad 20), ADC Battery input. GPIO signals are relative to this Voltage.
VDDA: Analog Supply Voltage
VCC: RF Supply Voltage

Is is recommended to connect VDDP, VDDB, VDDH, VDDA and VCC together.
Supply a voltage between 1.755 V and 3.63 V.
Add a 1 uF decoup. cap. to VDDP, VDDH, VDDA, VCC each. Add a 2.2 uF decoup cap. to VDDB.

=== Pins only with decoupling capacitor ===
VDDS: High Voltage Digital Supply. Add a 2.2 uF decoup. cap. rel to VSS.
VDDC: SIMO Buck Converter Voltage Core Output Supply. Add a 2.2uF decoup. cap. rel. to VSSP
VDDF: SIMO Buck Converter Voltage Flash/Memory Output Supply. Add a 2.2uF decoup. cap. rel. to VSSP.
DVDD: Decoupling Cap for BLE Energy Supply. Add a 47 nF decoup Cap.
VDCDCRF: BLE (RF) reference voltage. Add 1 uF decoup. cap. rel to VSSB

VDDC, VDDF and VDDS have a 2.2uF cap each. DVDD has a 47 nF cap. VDCDCRF has a 1 uF cap.

Connect VDCDCRF to VDDBH (directly or 0 Ohm resistor).

=== Pins with VSS Connection ===
VSSP: Ground Connection for SIMO Buck Converter
VSSA: Ground Connection for Analog Supply
VSSB: Ground Connection for BLE/Burst Buck Converter
VSS: Ground Connection for Digital. Source for Pad 37 and 41 LS power switch
VSSBA: Ground Connection for BLE Analog Supply
VSSVCO: Ground Connection for BLE VCO Supply
VSSS: Ground for BLE RF Supply

=== ADC Reference ===
ADCVREF: ADC Reference Voltage. Add 470 nF decoup. cap. rel to VSSA

=== SIMO buck converter ===
SIMOBUCK_SW: SIMO Buck Converter Inductor Switch Output
SIMOBUCK_SWSEL: SIMO Buck Converter Inductor Switch Input.

Add a 2.2 uH Inductor between SIMOBUCK_SW and SIMOBUCK_SWSEL for SIMO buck operation.
No decoup. cap. is needed.

=== BLE/Burst Buck Converter ===
VDDBH_SW: BLE/Burst Buck Converter Inductor Switch
VDDBH: BLE/Burst Buck Converter Voltage Output Supply.

Add a 1 uH Inductor between VDDBH_SW and VDDBH for BLE/Burst Buck Converter operation.
Add a 4.7uF decoup. cap. rel between VDDBH and VSSB.

ETH
Eidgenössische Technische Hochschule Zürich
Swiss Federal Institute of Technology Zurich

Project: Application MCU Power

Drawing number: 5	Rev: 1	Format: A4 Q	Laboratory: Computer Engineering Group, TIK	Sheet: App_Power.SchDoc	
Date: 12/9/2021 1:15:06 PM			Drawn by: Luca Rufer	Page 5	of 10
File: Y:\EharvDPP_PCB\App_Power.SchDoc					

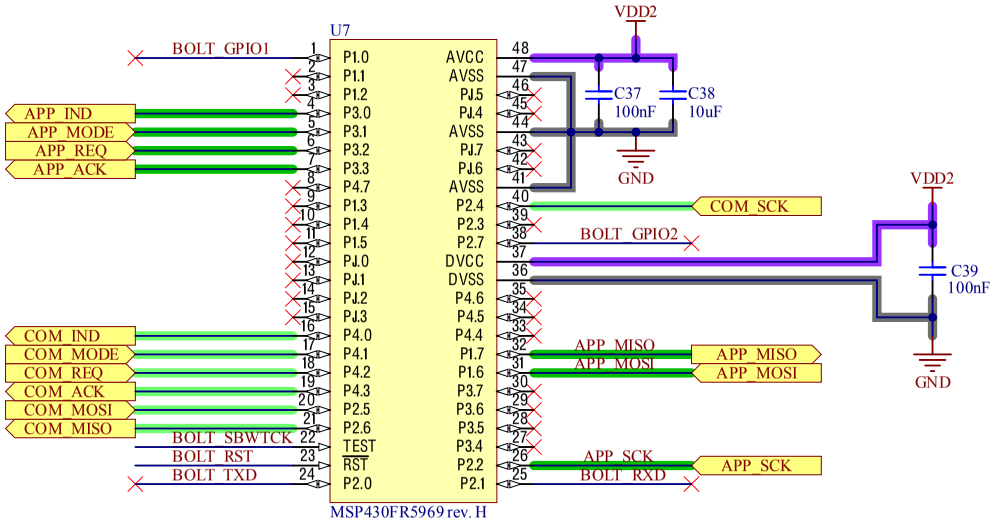

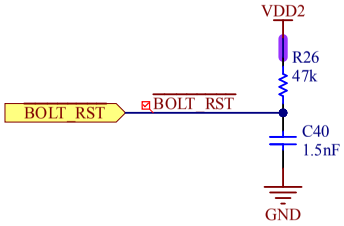

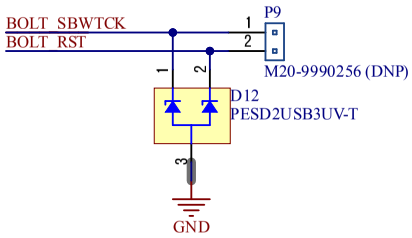

Note: The MSP430FR5969 MCU should be rev. H where errata PMM24 (lockup during wakeup from LPM4) has been fixed!

ETH Eidgenössische Technische Hochschule Zürich Swiss Federal Institute of Technology Zurich			Project: BOLT	
Drawing number: 6	Rev: 1.1	Format: A4 Q	Laboratory: Computer Engineering Group, TIK	Sheet: BOLT.SchDoc
Date: 12/9/2021 1:15:06 PM			Drawn by: Reto Da Forno	Page 6 of 10
File: Y:\EharvDPP_PCB\BOLT.SchDoc				

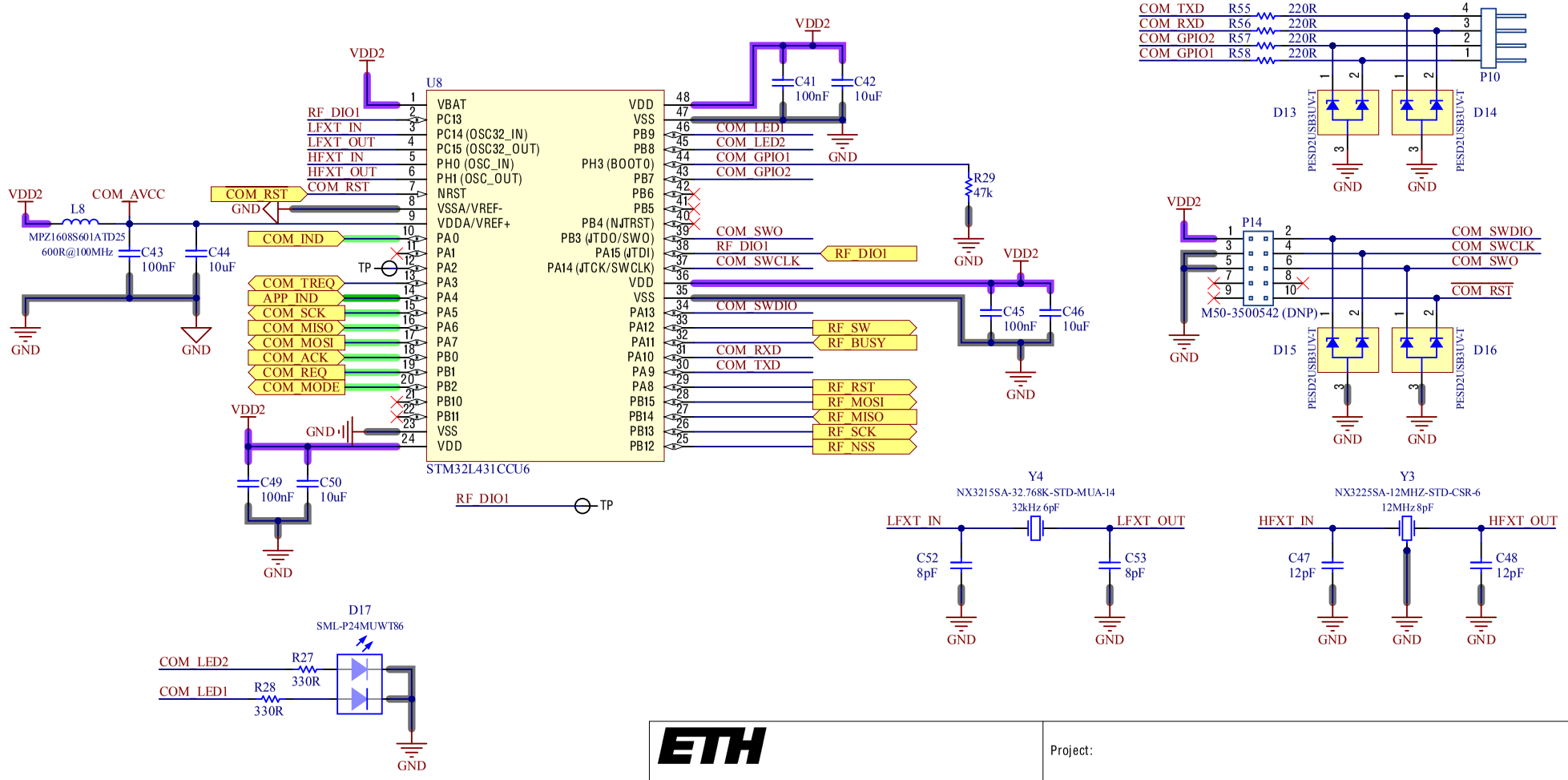

Eidgenössische Technische Hochschule Zürich Swiss Federal Institute of Technology Zurich			Project: STM32L4 Microcontroller	
Drawing number: 7	Rev: 1	Format: A4 Q	Laboratory: Computer Engineering Group, TIK	Sheet: Comm.SchDoc
Date: 12/9/2021 1:15:06 PM			Drawn by: Reto Da Forno	Page 7 of 10
File: Y:\EharvDPP_PCB\Comm.SchDoc				

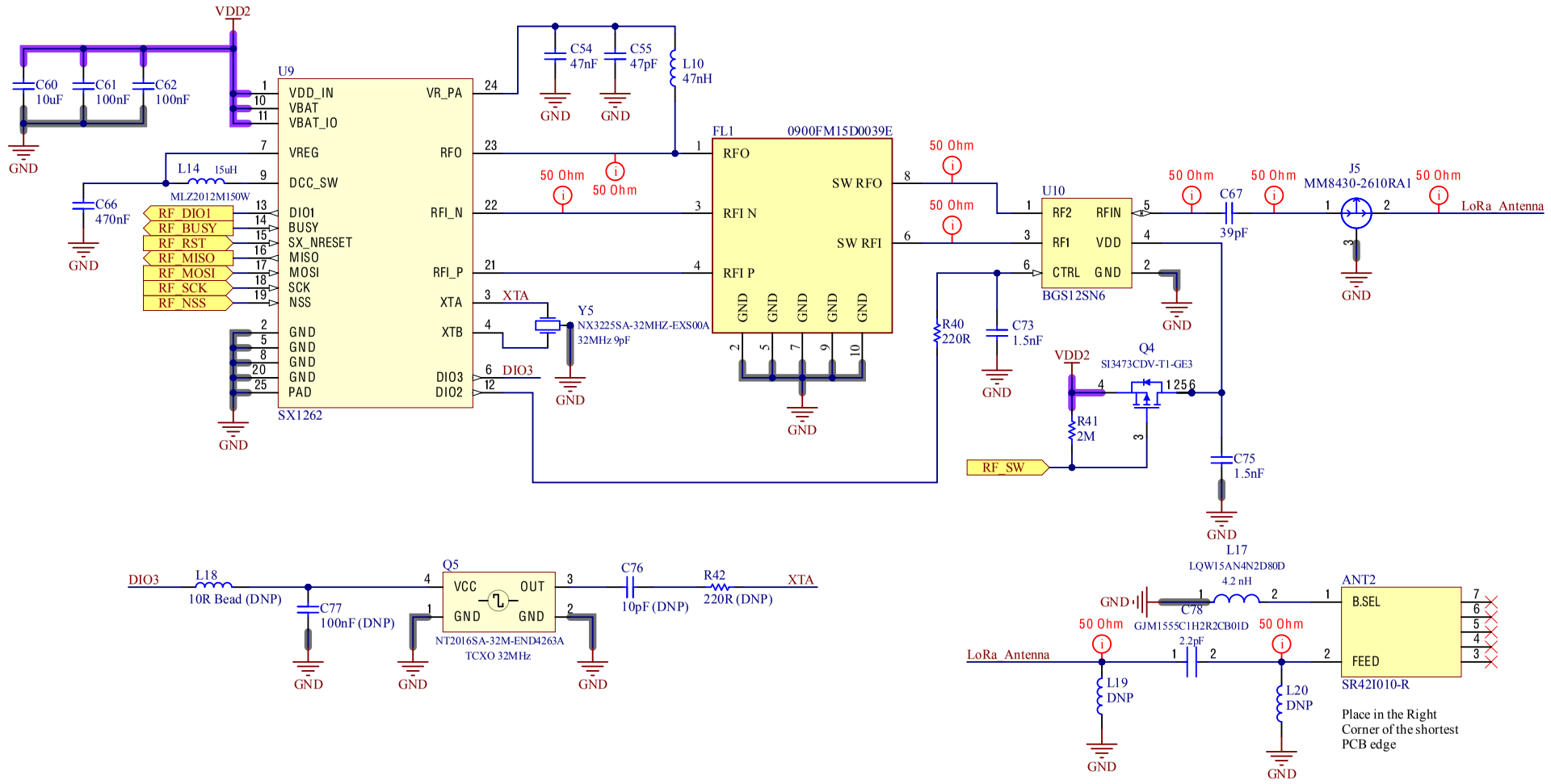

ETH Eidgenössische Technische Hochschule Zürich Swiss Federal Institute of Technology Zurich			Project: SX1262 868MHz Radio Transceiver		
Drawing number: 8	Rev: 1.1	Format: A4 Q	Laboratory: Computer Engineering Group, TIK	Sheet: Radio.SchDoc	
Date: 12/9/2021 1:15:06 PM			Drawn by: Reto Da Forno	Page 8 of 10	
File: Y:\EharvDPP_PCB\Radio.SchDoc					

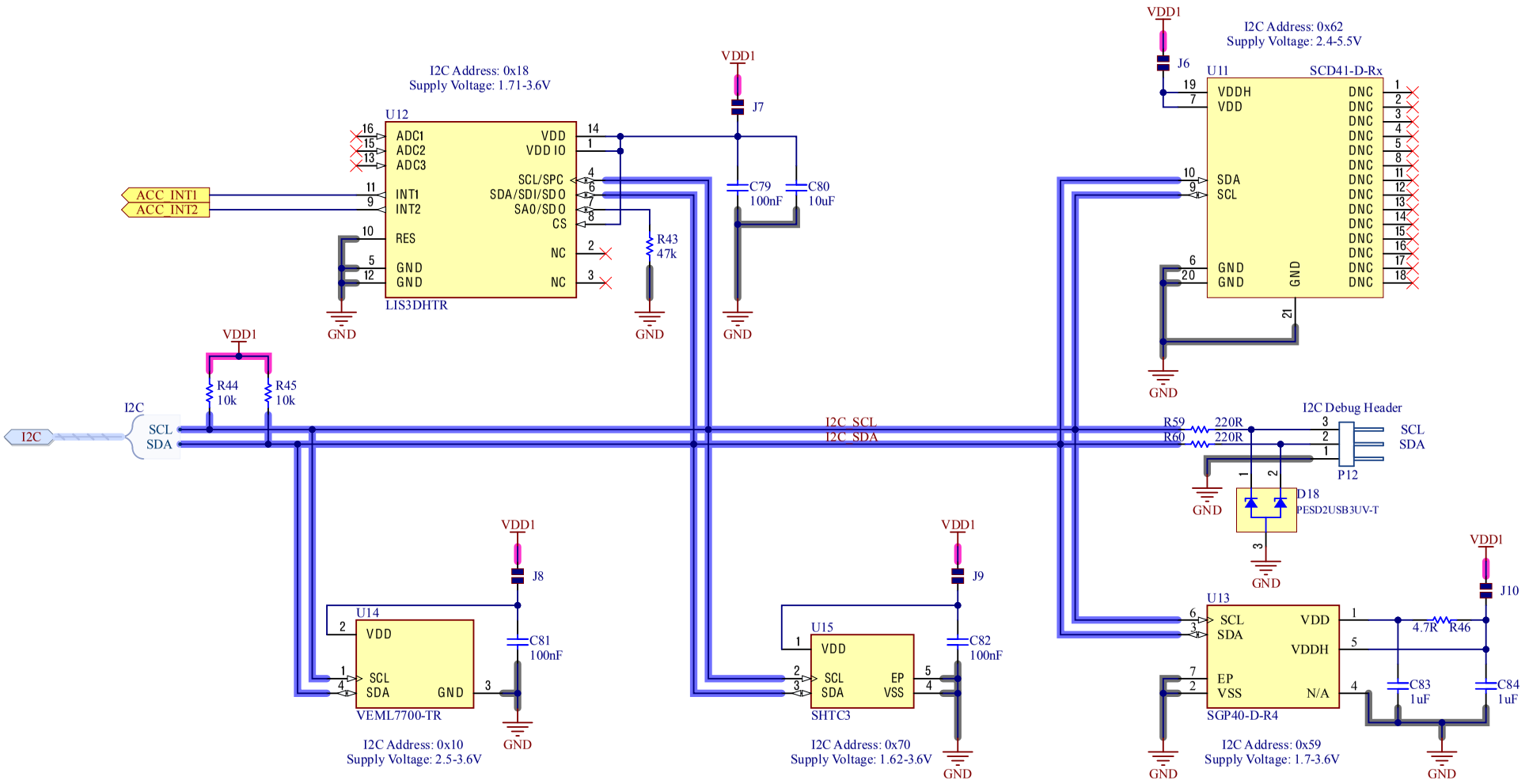

Note for Power Measurements:
If sensors are mounted, but the VDD1 jumper is open, it is still possible that current is leakes into the sensor over the SCL/SDA pins.

ETH

Eidgenössische Technische Hochschule Zürich
Swiss Federal Institute of Technology Zurich

Project: Sensors

Drawing number: 9	Rev: 1	Format: A4 Q	Laboratory: Computer Engineering Group, TIK	Sheet: Sensors.SchDoc	
Date: 12/9/2021 1:15:07 PM			Drawn by: Luca Rufer	Page 9 of 10	
File: Y:\EharvDPP_PCB\Sensors.SchDoc					

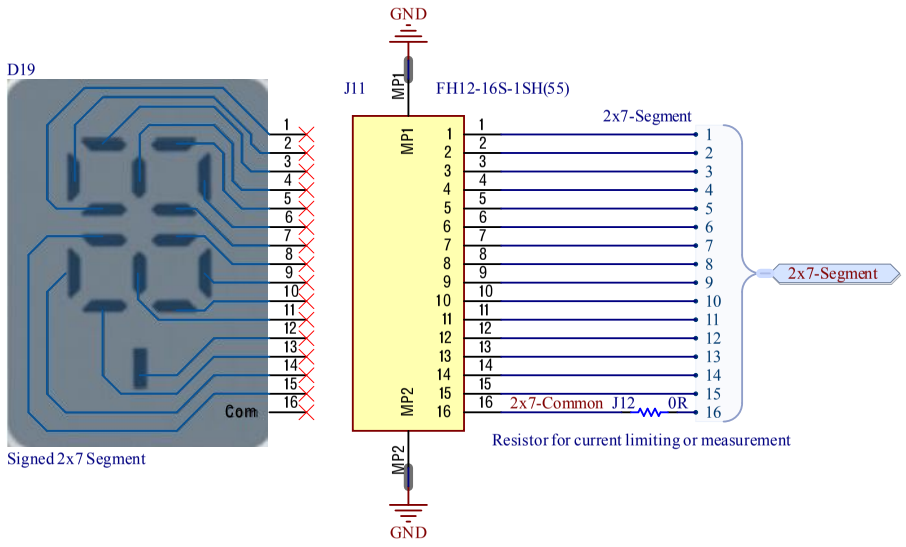

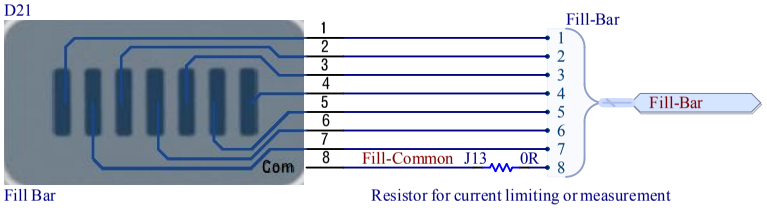

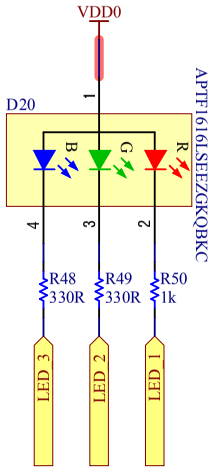

Eidgenössische Technische Hochschule Zürich Swiss Federal Institute of Technology Zurich	Project: Display and LEDs		
Drawing number: 10 Rev: 1 Date: 12/9/2021 1:15:07 PM	Format: A4 Q	Laboratory: Computer Engineering Group, TIK Drawn by: Luca Rufer	Sheet: Display.SchDoc Page 10 of 10
File: Y:\EharvDPP_PCB\Display.SchDoc			

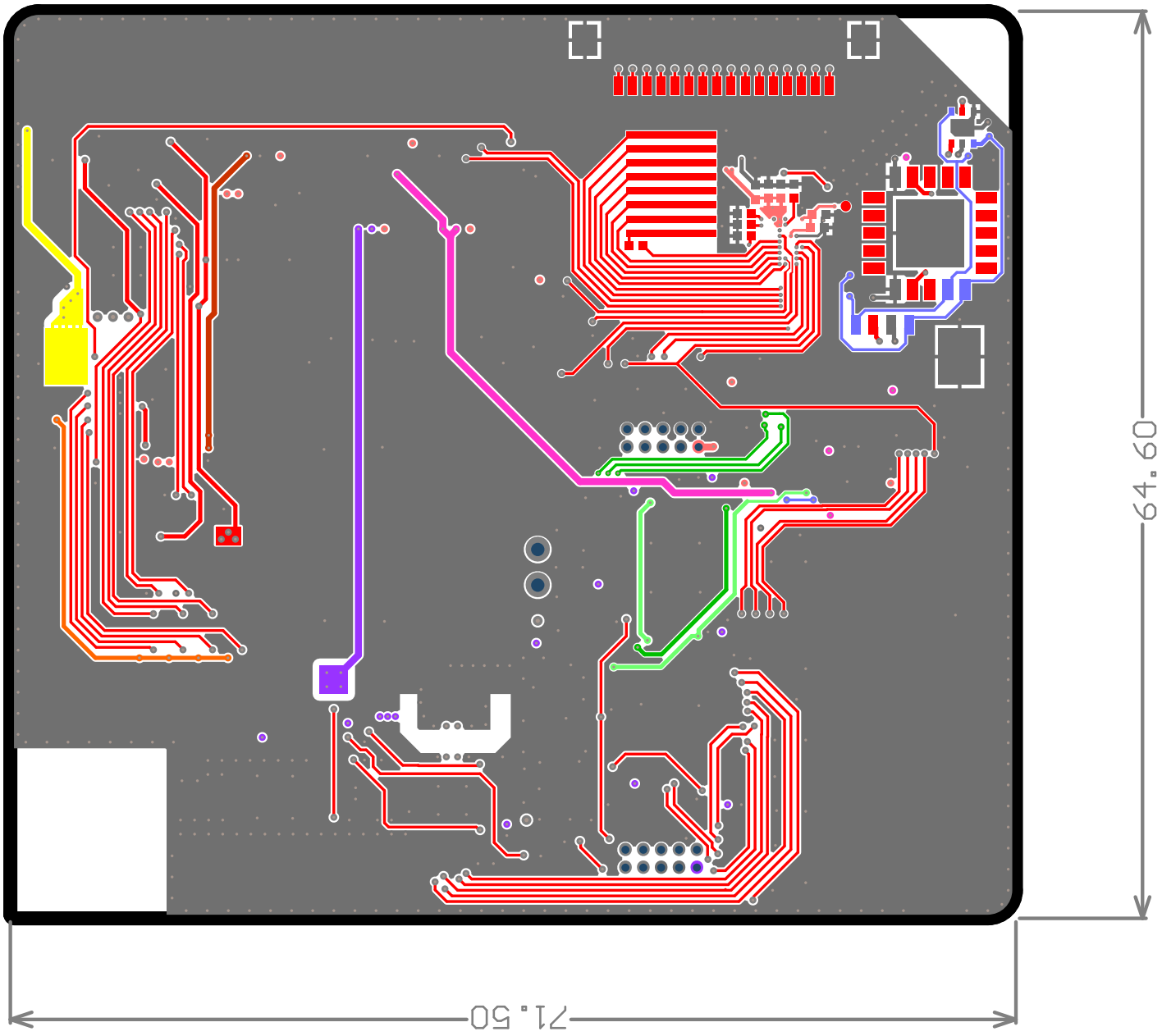
64.60
71.50

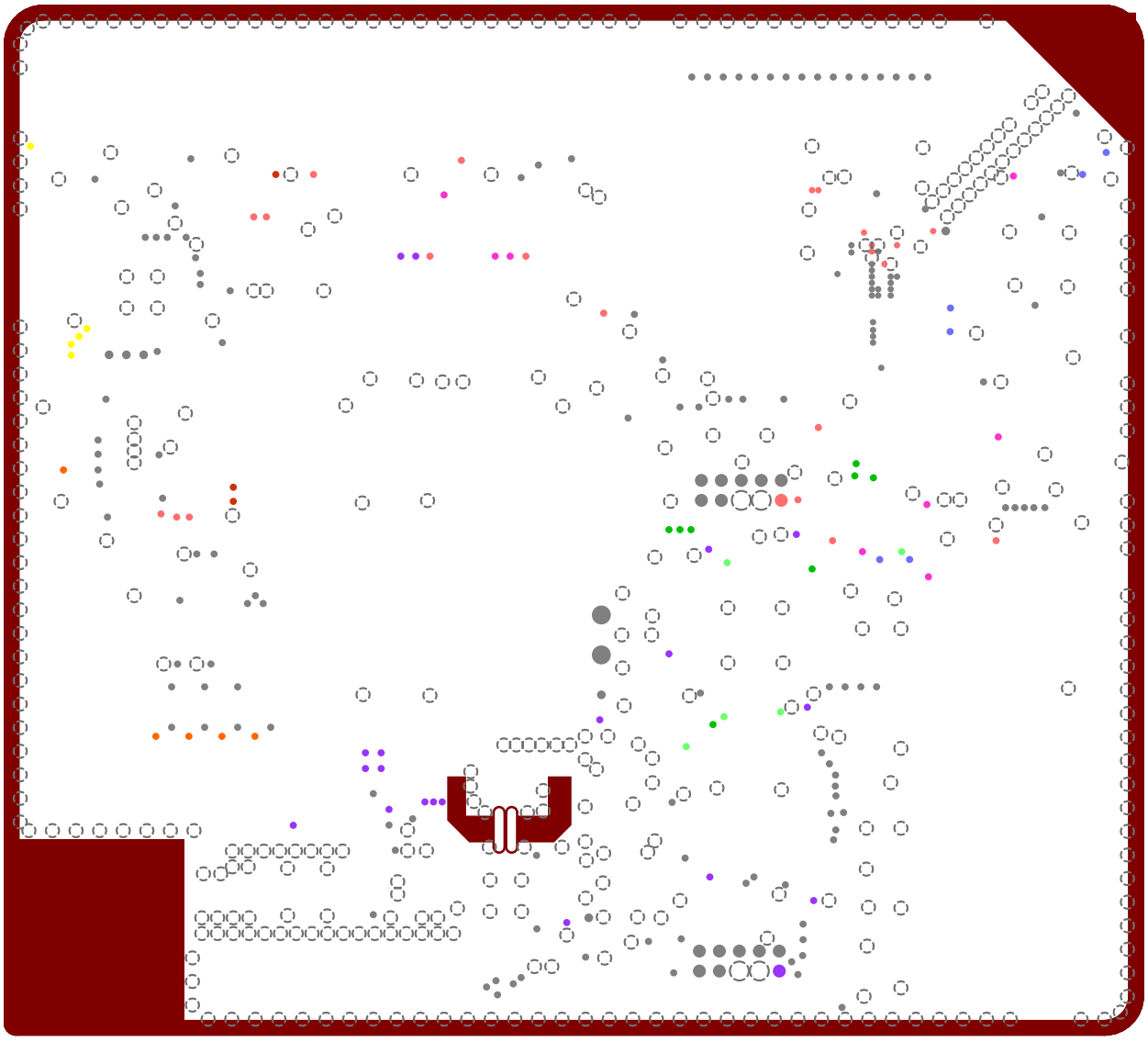

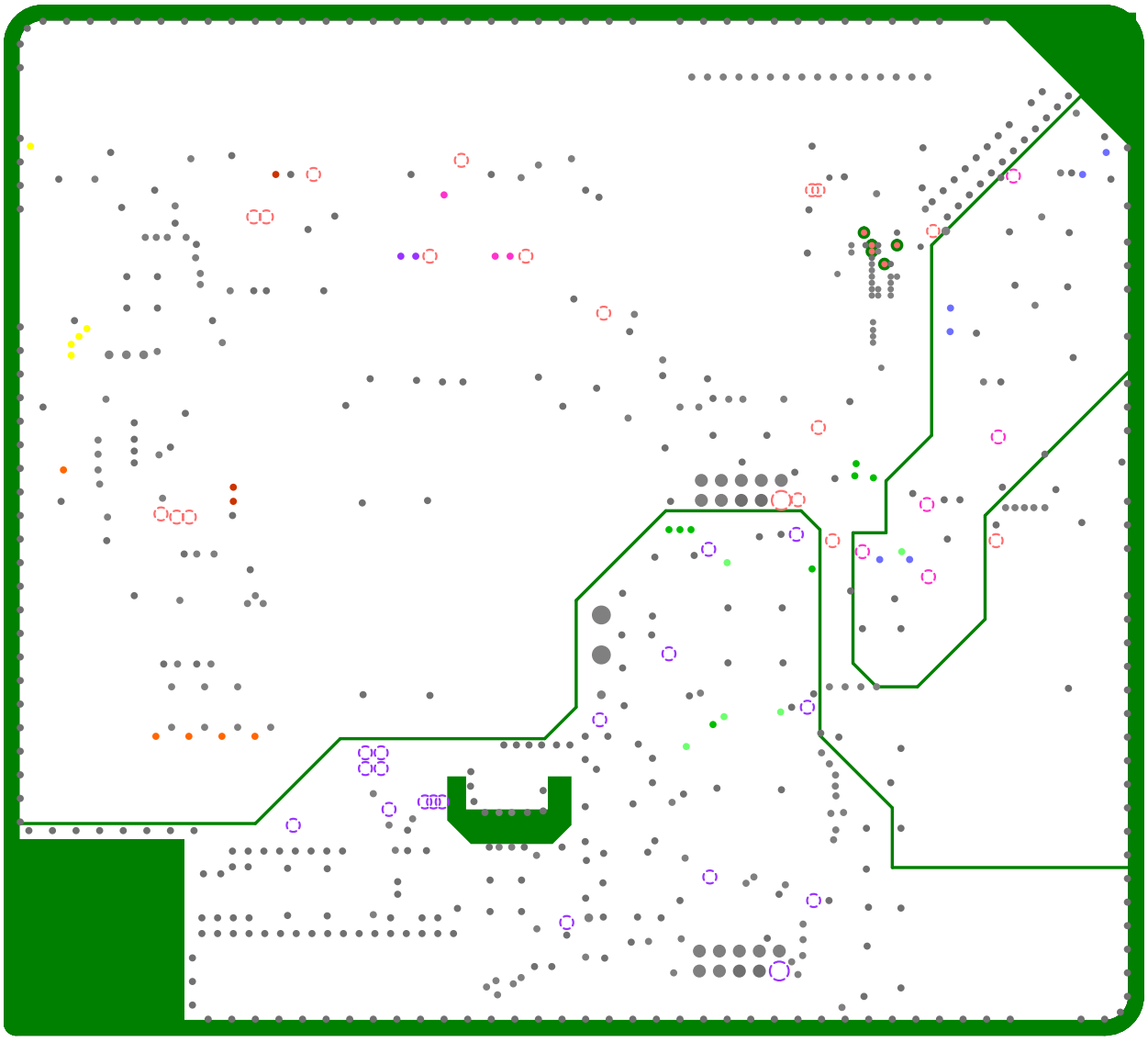

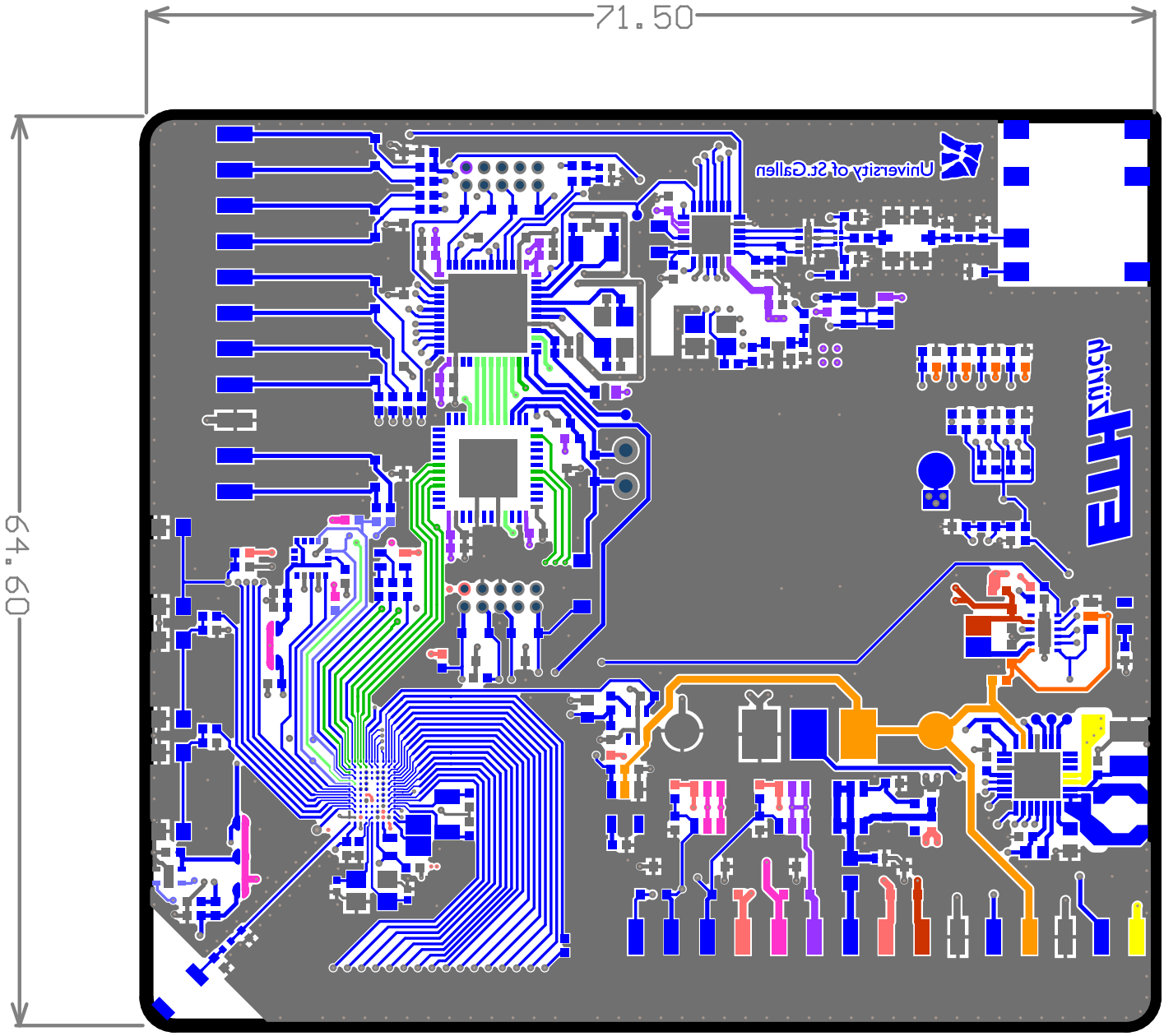
71.50
64.60
University of St.Gallen


J11
U13
D21
C29
C25
C28
C33
TP4
C36
C35
C32
C30
C27
U13
U11
U14
PS1

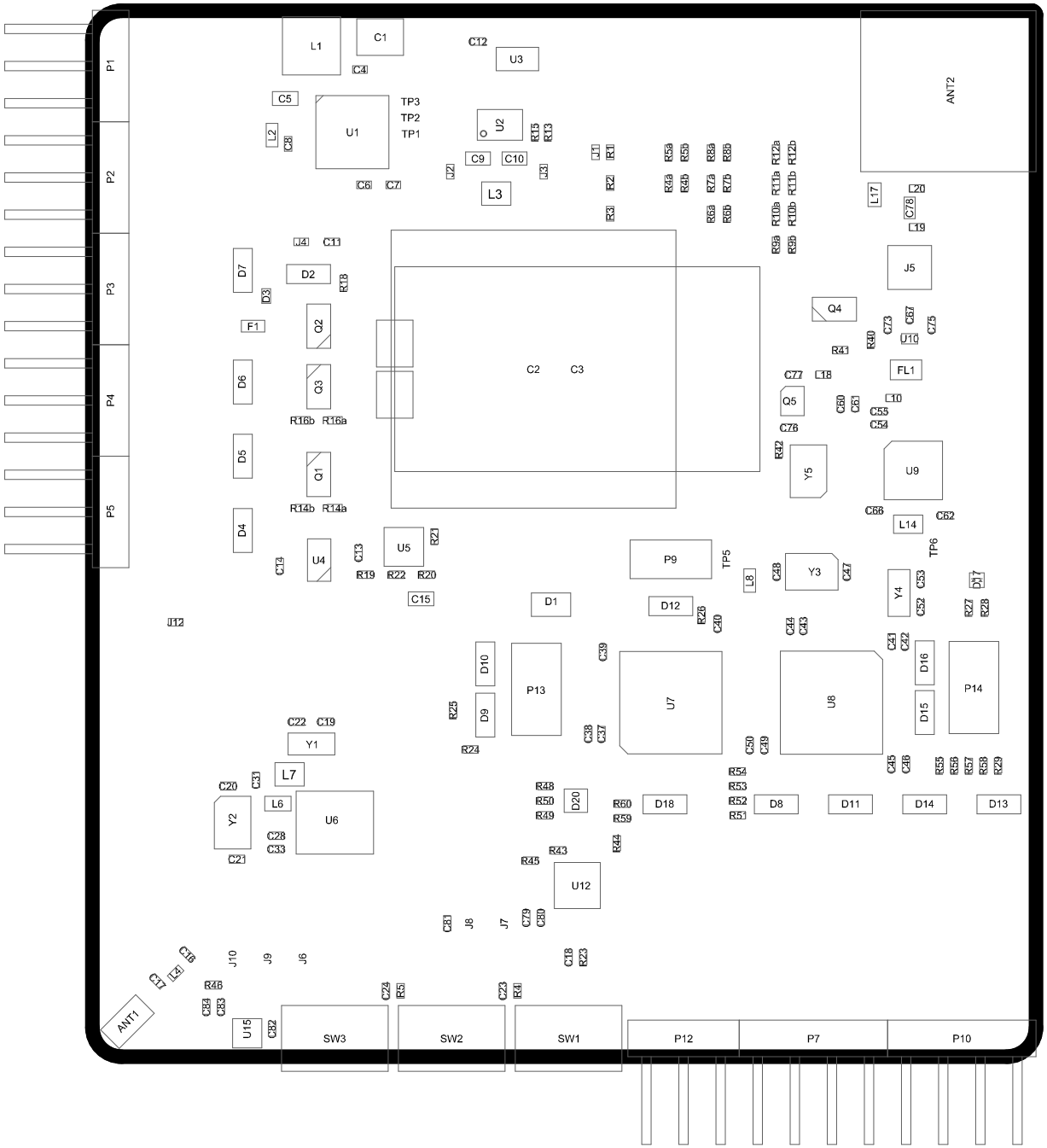
P1
P2
P3
P4
P5
L1
C1
C4
C12
U3
ANT2
C5
U1
TP3
TP2
TP1
U2
L2
C8
C9
C10
C6
C7
L3
J1
J2
J3
R1
R2
R3
R5a
R5b
R8a
R8b
R12a
R12b
R4a
R4b
R7a
R7b
R11a
R11b
R6a
R6b
R10a
R10b
R9a
R9b
L17
L20
C78
L19
J4
C11
D7
D2
R19
D3
F1
Q2
J5
Q4
C73
C67
C75
U10
R40
R41
C2
C3
C77
L18
FL1
Q5
C60
C61
L10
C55
C54
C76
R42
Y5
U9
C66
C62
L14
TP6
D6
Q3
R16b
R16a
D5
Q1
R14b
R14a
D4
U4
C13
U5
R21
C14
R19
R22
R20
C15
P9
TP5
L8
C48
Y3
C47
Y4
C53
D17
C52
R27
R28
J12
D1
D12
R26
C40
C44
C43
C41
C42
D16
P14
D10
P13
C39
U7
U8
D15
D9
R25
C38
C37
C50
C49
C45
C46
R55
R56
R57
R58
R29
R54
R53
R52
R51
C22
C19
Y1
L7
C20
C31
L6
Y2
U6
C28
C33
C21
R48
R50
R49
D20
R60
R59
D18
D8
D11
D14
D13
R43
R44
R45
U12
C81
J8
J7
C79
C80
C18
R23
C16
C17
L4
J10
J9
J6
R46
C84
C83
C24
R5
C23
R4
ANT1
U15
C82
SW3
SW2
SW1
P12
P7
P10

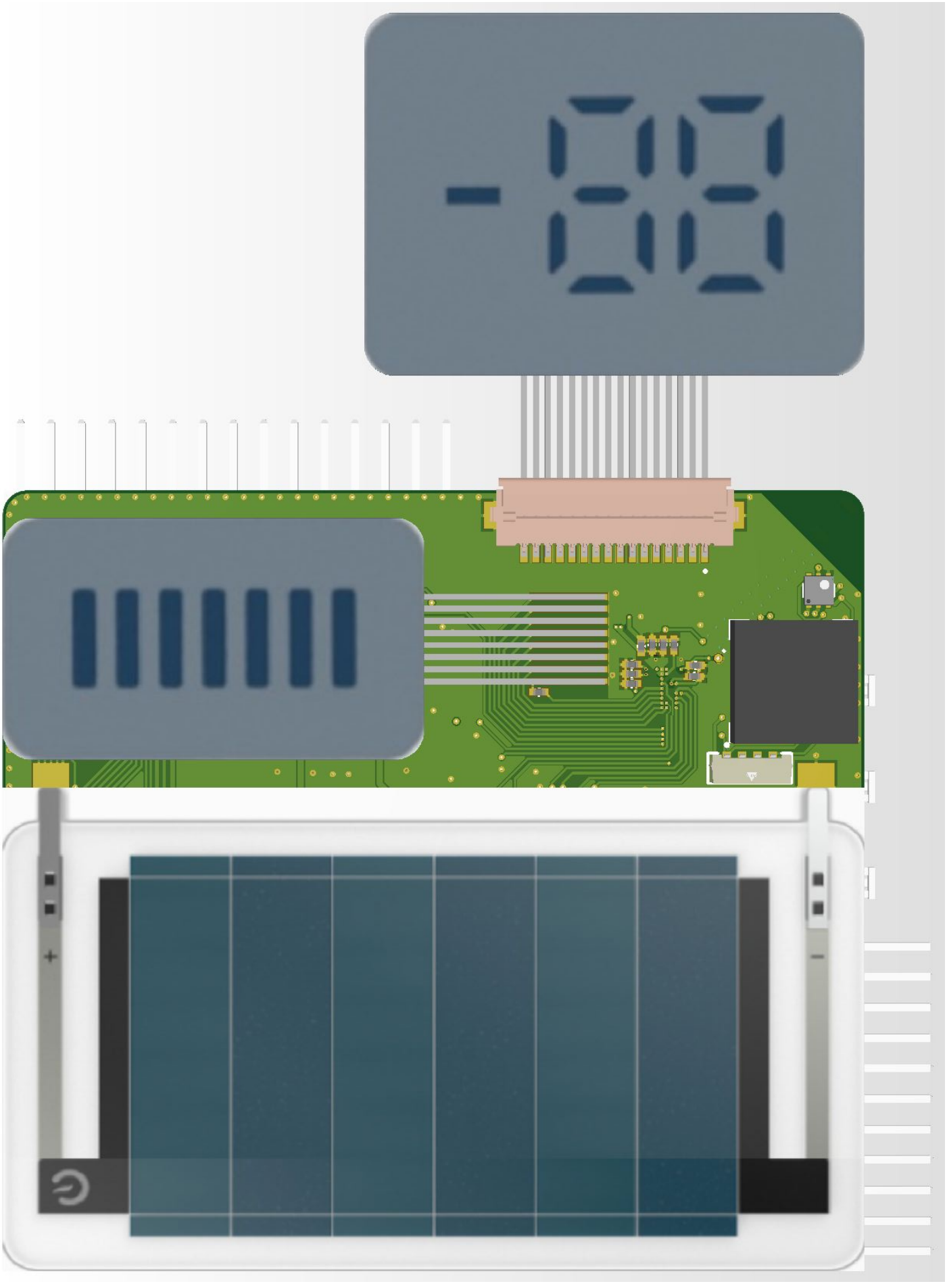

University of St.Gallen
ETH Zürich
CAP-XX
Energy Harvesting DPP
rev 1.0, 2021
COMM
APP
SENS
BOLT
PRIM
MPP
CFG
VSEL
STS
BAL
RESET
APP2
APP1
GPIO1
GPIO2
RX
TX
GND
SDA
SCL
TXEN
VSOL
VPRIM
GND
VBAT
BAL
GND
VBUCK_OUT
VDD0
VEXT
VDD2
VDD1
VDD0
VDD2EN
VDD1EN
VDD0EN

Commissioning Document

Harvesting-Based DPP for Indoor Environmental Monitoring

Commissioning Document

Select Board Configuration

The Harvesting-Based DPP for Indoor Environmental Monitoring offers multiple configurable options for Energy storage, supply voltage and more. Depending on the option, different components need to be added to the board, as listed below. For configuration of some components, external resistors for pull-up or pull-down are required. Such resistor pairs are labelled with Designators Rxa and Rxb for pull-up and pull-down, respectively. There is at most one Resistor of each pair mounted.

Maximum Power Point Tracking

The energy harvesting chip can be configured for different maximum power points of the solar panel, as listed in the table below. According to the datasheet of the solar panel, the maximum power point of the solar panel is between 80% and 85%. Thus, MPPT selection 2 is recommended (mount resistors R4b, R5a).

Maximum Power Point Tracking	Resistor Configuration
70%	0: R4b, R5b
75%	1: R4a, R5b
85% (Recommended)	2: R4b, R5a
90%	3: R4a, R5a

Energy Storage

The HBDPP board has multiple options for energy storage: On the PCB, there are footprints for two different supercapacitors or a 2S-Battery configuration. The footprints for the components overlap and thus only one of the three options can be used. As an alternative, an external Energy Storage can be connected to pin header P2. The table below lists the different options, their voltage limits, maximum Energy Storage and which resistors are recommended to be mounted for each component. More information about the configuration can be found in the AEM10941 Datasheet.

Part	Capacity	Min. Voltage	Max. Voltage	Est. Max. Energy[1]	Recommended AEM config
GA209F	90 mF	0 V	5.5 V	0.744 J[2]	3: R6a, R7a, R8b

[1] Maximum Energy storage of the component when connected to the E-peas AEM10941 Harvesting Chip (Energy Source) with optimal configuration (max output of 4.5 V) and the TPS62740 Buck converter (Energy Drain with a minimum input voltage of 2.2V). The efficiency of the buck converter is not considered.

[2] Capacitor Energy $E = 0.5 \cdot C \cdot (V_{max}^2 - V_{min}^2)$ between fully charged ($V_{max} = 4.5\ V$ due to AEM limit) and discharged ($V_{min} = 2.2\ V$ due to buck limit).

DMT3N4R2U224M3DTA0	220 mF	0 V	4.2 V	1.460 J[3]	7: R6a, R7a, R8a
ITX121010A (2s config.)	100 µAh	3 V	5.4 V	1.08 J[4]	3: R6a, R7a, R8b

Note:

- The Battery Configuration also needs another voltage supervisor with a voltage threshold of 3V (e.g. BU4330G-TR) to prevent discharging the batteries too far.
- Do not connect the solar panel to the AEM harvester if no power storage component is present!
- If an external component is connected which does not use the Balance pin, this pin has to be tied to ground using a jumper cable or soldering a 0Ω jumper in place of BAT2.

Primary Battery

If the solar panel is unable to provide enough power to the circuitry, an additional primary battery can be connected to the AEM harvesting chip as a backup. This battery can be connected using Pin header P1. If this functionality is to be used, the PCB must be configured with different components as specified in the table below. Components that are not used are marked with DNP (Do not place). When the Primary Battery is used, the Resistors R1 and R2 must be selected depending on the Battery, as stated in the AEM10941 Datasheet. For a Li-ion Battery that can be discharged to 3.3 V, Resistor values of R2 = 180 kΩ and R1 = 300 kΩ are recommended.

Primary Battery	C1	C4	J1	R1	R2	R3
Not Used (recom.)	DNP	10 µF	0 Ω	DNP	0 Ω	0 Ω
Used	150 µF	DNP	DNP	Dep. on Battery		DNP

Before connecting the battery, make sure that J1 is not connected. Otherwise, the battery will be short-circuited!

Application Circuit Operating Voltage

The operating voltage of the rest of the circuit can be selected between 1.8 V and 3.3 V, in steps of 100 mV. While most of the ICs on the PCB can be powered with 1.8 V, some sensors require a minimal Voltage of 2.5 V (See Schematics for supply ranges). If these sensors are not used, the board can be powered with lower voltages to use the energy storage components more efficiently. Note that the buck converter will be shut down when its supply voltage falls below 1.925 V, unless it is disabled at a higher voltage by the voltage supervisor.

Supply Voltage	R9y	R10y	R11y	R12y	Supply Voltage	R9y	R10y	R11y	R12y
1.8 (recom.)	b	b	b	b	**2.6**	a	b	b	b
1.9	b	b	b	a	**2.7**	a	b	b	a
2.0	b	b	a	b	**2.8**	a	b	a	b
2.1	b	b	a	a	**2.9**	a	b	a	a
2.2	b	a	b	b	**3.0**	a	a	b	b

[3] Capacitor Energy $E = 0.5 \cdot C \cdot (V_{max}^2 - V_{min}^2)$ between fully charged ($V_{max} = 4.12\ V$ which is the closest AEM setting below the capacitors voltage limit) and discharged ($V_{min} = 1.925\ V$ due to buck limit).

[4] The battery cannot be fully charged using the AEM and thus only reaches approx. 75% of its maximum charge. Two Batteries at an average voltage of $V_{avg} = 2\ V$ and a capacity of $75\mu Ah$ have a maximum Energy of $E = 2 \cdot V \cdot It$.

2.3	b	a	b	a	**3.1**	a	a	b	a
2.4	b	a	a	b	**3.2**	a	a	a	b
2.5	b	a	a	a	**3.3**	a	a	a	a

Power domain enable

All parts on the PCB that are not part of the harvesting and energy storage circuit belong to one of three power domains. Domain 0 consists out of the Apollo 3 Plus Application Processor (APP), the Bluetooth low Energy module (part of the APP processor) and the Electrochromic display. Domain 1 contains the sensors and domain 2 contains BOLT, the communication processor (COMM) and the LoRa Transceiver. Power domain 0 is always on when the buck converter is providing power. Power domains 1 and 2 are enabled by the application processor. The Power domains can be set as normally-on or normally-off (when the APP processor is powered down) using configuration resistors as shown in the table below.

Power domain 1	**R14a**	**R14b**	**Power domain 2**	**R16a**	**R16b**
Normally-off (recom.)	2 MΩ	DNP	**Normally-off** (recom.)	2 MΩ	DNP
Normally-on	DNP	2 MΩ	**Normally-on**	DNP	2 MΩ

Temperature compensated oscillator for LoRa

To increase the performance of the LoRa communication for a wider range of temperatures, a temperature-controlled oscillator can be used instead of the normal oscillator. The parts used for this are listed in the table below.

LoRa Oscillator	**Y5**	**Q5**	**L18**	**C76**	**C77**	**R42**
Normal (recom.)	NX3225SA	DNP	DNP	DNP	DNP	DNP
Temperature comp.	DNP	NT2016SA	10 Ω Bead	100 nF	10 pF	220 Ω

Pin Headers

The PCB has a total of 11 Pin headers. Pin header P9 is used to program BOLT and has a smaller hole diameter to fit a pin header that makes contact without soldering it to the board permanently, as the BOLT processor ideally only has to be programmed once. Pin headers P13 and P14 are used for programming the application processor and the communication processor, respectively. They also have a smaller hole diameter to temporarily fit the pin header without having to solder it. However, the holes are still big enough that the connector has to be held at an angel to make contact during programming.
All other pin headers are SMD pin headers at the edge of the board. These pin headers are intended to be used for measurements and debugging. If the pin headers are not added to the board, the SMD pads can be used as test points.

Header	**Pin 1**	**Pin 2**	**Pin 3**	**Pin 4**	**Usage**
P1	GND	V_{prim}	V_{sol}	-	Measure solar panel, connect primary battery
P2	GND	$V_{Balance}$	V_{bat}	-	Measure voltage of battery (or Supercap) and mid-voltage balancing pin, or connect an external energy storage component.

P3	V_{ext}	V_{DD0}	V_{buck_out}	-	Supply external power to the circuit over a protected input, or measure the output of the buck converter and the power domain 0 voltage. If jumper J3 is not mounted, a jumper can be placed between pin 2 and 3 to power V_{DD0} from the buck converter. In this case, make sure that V_{ext} is not connected.
P4	V_{DD0}	V_{DD1}	V_{DD2}	-	Measure the voltages of the different power domains.
P5	V_{DD0_EN}	nV_{DD1_EN}	nV_{DD2_EN}	-	Measure which power domains are enabled. Note that for domain 1 and 2, the enable signal is active low.
P7	APP_{GPIO1}	APP_{GPIO2}	APP_{RX}	APP_{TX}	Connect to two programmable GPIOs of the application processor and used for UART communication with the Application Processor. Connect APP_{RX} to Tx of your device and vice versa.
P9	$BOLT_{SBWTCK}$	$BOLT_{RST}$	-	-	Pins used to program BOLT.
P10	COM_{GPIO1}	COM_{GPIO2}	COM_{RX}	COM_{TX}	Connect to two programmable GPIOs of the communication processor and used for UART communication with the communication Processor. Connect COM_{RX} to Tx of your device and vice versa.
P12	GND	SDA	SCL	-	Interface to the I^2C Sensor bus.

It must be made sure to NOT apply external power to the circuit when V_{buck_out} is connected to VDD0. The buck converter pulls its output to GND if its input voltage is too low. If the buck converter is active, it will try to regulate the externally supplied voltage to its voltage setpoint. In any case, the external voltage supply will be disturbed when connected to the output of the buck converter, which may damage the external supply or the buck converter.

Sensors

There is a total of 5 sensors which can be mounted on the PCB. The name of the sensors and their supply voltage range are given in the Schematics. If a sensor is not to be mounted, the surrounding components (decoupling capacitors, configuration resistors etc.) can be left out. Depending on which sensors are being used, the supply voltage can be adjusted to the minimum allowed, according to the table in “Application Circuit Operating Voltage”.

Jumpers

In addition to the Jumper J1, which is used to disable the primary battery, another three 0-Ω-Jumpers are used to divide the harvesting and power circuits into multiple parts to allow for easier testing and commissioning. In the beginning of the commissioning, all of these are supposed to be open.

Furthermore, there solder jumpers J6 to J10 can be used to enable and disable sensors. These are also not to be soldered at the beginning of the commissioning.

Jumper	Use
J1	Connect harvester's PRIM pin to GND. Used if no external battery is connected.
J2	Connects V_{bat} to the buck regulator's input.
J3	Connects the output of buck regulator to V_{DD0}.
J4	Connects external voltage supply to V_{DD0}.

Commissioning

The commissioning of the Harvesting Based DPP PCB will be done in multiple steps. The important steps are listed in boxes to provide a better overview. The text next to the boxes is used to provide some additional information about the steps.
The first step of the commissioning is to decide which configuration of the HBDPP is to be used. A guide for this can be found in the previous chapter.

1. Select board configuration

All configuration parts and all other bottom-side SMD components except the components listed below are to be soldered using the reflow oven.

2. Solder all SMD components on the bottom side of the PCB using the reflow oven, **except**:
   - The components not selected in the configuration
   - J2, J3, J4
   - All Pinheaders (P1 – P14)
   - Energy Storage Components (C2, C3, BAT1, BAT2)
3. Solder the remaining components for the Apollo circuit on the top side of the PCB (preferably bay hand):
   C25, C26, C27, C29, C30, C32, C34, C35, C36, J11 and J13.

Note that some components have special requirements for soldering:
ANT2 (SR42I010-R): 240°C maximum soldering temperature (255°C for lead-free). Use flux below the BGA package of the Apollo to get good soldering connections.
After soldering, the PCB must be checked for short circuits.

4. Check all pads of the power pin headers (P1-P5) to GND for short-circuits. Visually inspect all other solder joints.

Depending on the selected configuration, V_{PRIM} should be connected to GND if no primary battery will be connected. The V_{buck_out} Pin may show a low resistance of around 30 Ω, as the buck converter has an active discharge.

5. Mount the pin headers depending on the configuration.

Depending on which parts of the PCB will be used, not all pin headers are required to be soldered. To make the commissioning process easier, it is recommended to mount at least P2, P3, P7, P10.

Power Circuit

The first sub-circuit to be tested is the power circuit. When connecting to the pin headers, remember that the silk labels belong to the pin above them.

6. Apply 3.3V to the V_{ext} Pin and measure if there's 3.3 V between J4 (right Pad) and GND.

Optionally, the external supply with reverse voltage protection can be stress-tested with the following steps:
Before soldering J4, apply a negative voltage (e.g. -3.3 V) to the V_{ext} Pin and check that there is no negative voltage between J4 (right Pad) and GND.

7. Solder J4.

After soldering J4, connect a 10 Ω resistor (rated with 1W) between V_{DD0} and GND. Then supply 3.3 V to the V_{ext} Pin. Check the voltage at V_{DD0} and the voltage drop of the PFET and fuse by measuring V_{ext} to V_{DD0}. Under normal conditions, the resistance of the Fuse and the PFET should be about 100 mΩ and thus the expected voltage drop is 33 mV.

The next circuit to be tested is the buck converter. To make it easier to test the circuit, the Jumper J2 is soldered, so the input of the buck converter can be accessed via the V_{Bat} Pin. To measure some of the status signals in the next steps, a voltage has to be applied to V_{ext} for the pull-up of the signals to work.

8. Solder J2.
9. Apply 3.3 V to V_{ext} for the next few steps.
10. Apply 2 V to V_{Bat} and measure that V_{Buck_out}, V_{DD0_EN} and V_{DD0_PG} are all at 0 V.
11. If the selected output voltage is above 2.2V, increase the voltage to a level between 2.2 V and the selected output voltage. Measure that V_{DD0_EN} is high and that V_{Buck_out} and V_{DD0_PG} are still at 0 V.
12. Increase the voltage to the selected output voltage (but 2.2V minimum). Measure that V_{DD0_EN}, V_{Buck_out} and V_{DD0_PG} are all high. Measure that V_{Cap_full} is low.
13. Increase the voltage further to above 4 V. Measure now that V_{DD0_EN} is high (V_{Bat} voltage level), V_{Buck_out} is at the selected voltage, and V_{Buck_out}, and V_{DD0_PG} are high (at the voltage level supplied to V_{ext}).

Note that depending on the energy storage component that will be mounted later, other voltage supervisors (U3 and U4) are required. In this case, the values above need to be adapted to the threshold voltages of the new voltage supervisors. For the supercapacitors, U3 is not necessary and a 0Ω resistor can be placed between pads 1 and 2 of the U3-footprint to have the buck converter always enabled and get the most energy out of the storage compoenets.

Harvesting Circuit

After the power circuit was tested, the harvesting circuit is next. It is recommended to first check again if the Components J1, R1, R2, R3, C1 and C4 are soldered according to the selected configuration and have the correct values.

14. Solder the energy storage component.
15. Solder the solar panel.

16. Measure that V_{Buck} is 2.2 V when the solar panel is illuminated.
17. Measure at V_{Sol} if the harvester correctly performs the MPP tracking (requires an oscilloscope).
18. Measure if V_{Bat} increases at least to 2.2 V, optimally to the OV setting of the harvester configuration.
19. Check that $V_{Balance}$ is at $V_{Bat}/2$.
20. Check that the Testpoint STS 0 is high (V_{Bat}) once the storage component is charged above the V_{chrdy} set in the configuration.

The energy storage components must be soldered with care:
C2: Only solder with Aluminium solder and a manual soldering iron (<70W, 380°C max).
C3: Only solder with Sn-3Ag-0.5Cu, resin flux-cored solder wire and a manual Soldering iron (<70W, 350°C) for 3-4 seconds.
BAT1, BAT2: Special reflow soldering profile with 170°C maximum soldering temperature.
Pin headers: Can be soldered with reflow, but can also be soldered by hand.
Solar panel: The leads of the solar panel should only be heated for a short amount of time to prevent melting the plastic.

Apollo Circuit

21. Apply 3.3 V to V_{Ext} to power the Apollo.
22. Load the Blinky program using header P13.
23. Check that all functionalities of the Blinky program work.
24. Disconnect power and add the displays D19 and D21. Run the Blinky program again to check that the displays work correctly.
25. (optional) Load the BLE test program to verify the BLE functionality of the Apollo.
26. (optional) Load the deepsleep program and measure the current consumption.

Sensors

27. Solder the remaining sensors for the board configuration.
28. Close the solder jumpers (J6-10) for the sensors that will be used.
29. Connect 3.3 V to V_{Ext} and load the sensor test program on the Apollo.
30. Check that Power domain 1 is enabled (nV_{DD1_EN} is low) and that V_{DD1} has the correct voltage.
31. Check that all the sensors work correctly and return reasonable values.

Note that some sensors have a special soldering profile.
U11 (SCD41-D-R2): 235°C maximum soldering temperature.
U13 (SGP40-D-R2): 245°C maximum soldering temperature.

BOLT and Communication

32. Connect 3.3 V to V_{Ext} and load the comm test program on the Apollo.
33. Check that Power domain 2 is enabled (nV_{DD2_EN} is low) and that V_{DD2} has the correct voltage.
34. Program BOLT using P9.
35. Program the comm processor using P14.
36. Verify that the comm processor works correctly.

The Harvesting Based DPP is now fully commissioned.

Final remarks

As the device is always on, make sure the V_{BAT} Pin is not short-circuited during transportation. If changes are to be made to the configuration of the device, or external components are to be added, consult this document first to check if any other hardware modifications are necessary. If the device shall no longer be powered by an external source, solder J3 to connect the output of the buck converter. It is important that no external power is connected when J3 is closed. Thus, it is recommended to unsolder J4 if J3 is soldered.

Bibliography

[1] Andres Gomez. *On-Demand Communication with the Batteryless MiroCard: Demo Abstract*, page 629–630. Association for Computing Machinery, New York, NY, USA, 2020. ISBN 9781450375900. URL https://doi.org/10.1145/3384419.3430440.

[2] Jan Beutel, Roman Trüb, Reto Da Forno, Markus Wegmann, Tonio Gsell, Romain Jacob, Michael Keller, Felix Sutton, and Lothar Thiele. The dual processor platform architecture: Demo abstract. In *Proceedings of the 18th International Conference on Information Processing in Sensor Networks*, IPSN '19, pages 335–336, New York, NY, USA, 2019. ACM. ISBN 978-1-4503-6284-9. doi: 10.1145/3302506.3312481. URL http://doi.acm.org/10.1145/3302506.3312481.

[3] Felix Sutton, Marco Zimmerling, Reto Da Forno, Roman Lim, Tonio Gsell, Georgia Giannopoulou, Federico Ferrari, Jan Beutel, and Lothar Thiele. Bolt: A stateful processor interconnect. In *13th ACM Conference on Embedded Networked Sensor Systems (SenSys 2015)*, pages 267–280, Seoul, South Korea, 2015.

[4] Roman Trüb, Reto Da Forno, Markus Wegmann, Michael Keller, Andreas Biri, Tobias Gatschet, and Tobias Kuonen. Flora software, 2021. URL https://eth.swisscovery.slsp.ch/permalink/41SLSP_ETH/lshl64/alma99117766552205503.

[5] Markus Wegmann. Reliable 3rd generation data collection. Master's thesis, Computer Engineering and Networks Laboratory, Department of Information Technology and Electrical Engineering, ETH Zürich, 2018.

[6] Andreas Biri, Reto Da Forno, Tonio Gsell, Tobias Gatschet, Jan Beutel, and Lothar Thiele. Stec: Exploiting spatial and temporal correlation for event-based communication in wsns. In *Proceedings of the 19th ACM Conference on Embedded Networked Sensor Systems*, SenSys '21, page 274–287, New York, NY, USA, 2021. Association for Computing Machinery. ISBN 9781450390972. doi: 10.1145/3485730.3485951. URL https://doi.org/10.1145/3485730.3485951.

[7] Federico Ferrari, Marco Zimmerling, Luca Mottola, and Lothar Thiele. Low-power wireless bus. In *SenSys '12: Proceedings of the 10th ACM Conference on Embedded Network Sensor Systems*, SenSys '12, page 1–14, New York, NY, USA, 2012. Association for Computing Machinery. ISBN

9781450311694. doi: 10.1145/2426656.2426658. URL https://doi.org/10.1145/2426656.2426658.

[8] Felix Sutton, Reto Da Forno, David Gschwend, Tonio Gsell, Roman Lim, Jan Beutel, and Lothar Thiele. The design of a responsive and energy-efficient event-triggered wireless sensing system. In *Proceedings of the 2017 International Conference on Embedded Wireless Systems and Networks*, EWSN '17, page 144–155, USA, 2017. Junction Publishing. ISBN 9780994988614.

[9] Markus-Philipp Gherman, Yun Cheng, Andres Gomez, and Olga Saukh. Compensating altered sensitivity of duty-cycled mox gas sensors with machine learning. In *18th Annual IEEE International Conference on Sensing, Communication, and Networking (SECON 2021)*, 2021.

[10] Epishine. *Organic Indoor Light Energy Harvesting Modules Product Sheet*. Linköping, Sweden, 2021. URL https://uploads-ssl.webflow.com/5d9317a367afa8fe9ed01a09/60e2f318bf114d29ba5c714d_LEH3%20Product%20Brief.pdf.